Redox Biology 70 (2024) 103072

Contents lists available at ScienceDirect

Redox Biology

journal homepage: www.elsevier.com/locate/redox

Macrophage Tim-3 maintains intestinal homeostasis in DSS-induced colitis by suppressing neutrophil necroptosis

Fangfei Wang [a,b], Feng Zhou [a,b], Jianxiang Peng [a,b], Hao Chen [a,b], Jinliang Xie [a,b], Cong Liu [a,b], Huifang Xiong [a,b], Sihai Chen [a,b], Guohui Xue [c], Xiaojiang Zhou [a,b], Yong Xie [a,b,*]

[a] Department of Gastroenterology, Digestive Disease Hospital, The First Affiliated Hospital of Nanchang University, Jiangxi Medical College, Nanchang University, Nanchang, Jiangxi Province, China
[b] Institute of Digestive Disease, The First Affiliated Hospital of Nanchang University, Jiangxi Medical College, Nanchang University, Nanchang, Jiangxi Province, China
[c] Department of Clinical Laboratory, Affiliated Jiujiang Hospital of Nanchang University, Jiujiang, Jiangxi Province, China

ARTICLE INFO

Keywords:
Tim-3
Necroptosis
Neutrophil
Macrophage
ROS
Inflammatory bowel disease

ABSTRACT

T-cell immunoglobulin domain and mucin domain-3 (Tim-3) is a versatile immunomodulator that protects against intestinal inflammation. Necroptosis is a type of cell death that regulates intestinal homeostasis and inflammation. The mechanism(s) underlying the protective role of macrophage Tim-3 in intestinal inflammation is unclear; thus, we investigated whether specific Tim-3 knockdown in macrophages drives intestinal inflammation via necroptosis. Tim-3 protein and mRNA expression were assessed via double immunofluorescence staining and single-cell RNA sequencing (sc-RNA seq), respectively, in the colonic tissues of patients with inflammatory bowel disease (IBD) and healthy controls. Macrophage-specific *Tim3*-knockout (Tim-3^{M-KO}) mice were generated to explore the function and mechanism of *Tim-3* in dextran sodium sulfate (DSS)-induced colitis. Necroptosis was blocked by pharmacological inhibitors of receptor-interacting protein kinase (RIP)1, RIP3, and reactive oxygen species (ROS). Additionally, *in vitro* experiments were performed to assess the mechanisms of neutrophil necroptosis induced by Tim-3 knockdown macrophages. Although Tim-3 is relatively inactive in macrophages during colon homeostasis, it is highly active during colitis. Compared to those in controls, Tim-3^{M-KO} mice showed increased susceptibility to colitis, higher colitis scores, and increased pro-inflammatory mediator expression. Following the administration of RIP1/RIP3 or ROS inhibitors, a significant reduction in intestinal inflammation symptoms was observed in DSS-treated Tim-3^{M-KO} mice. Further analysis indicated the TLR4/NF-κB pathway in Tim-3 knockdown macrophages mediates the TNF-α-induced necroptosis pathway in neutrophils. Macrophage Tim-3 regulates neutrophil necroptosis via intracellular ROS signaling. Tim-3 knockdown macrophages can recruit neutrophils and induce neutrophil necroptosis, thereby damaging the intestinal mucosal barrier and triggering a vicious cycle in the development of colitis. Our results demonstrate a protective role of macrophage Tim-3 in maintaining gut homeostasis by inhibiting neutrophil necroptosis and provide novel insights into the pathogenesis of IBD.

1. Introduction

Inflammatory bowel disease (IBD) is a chronic immune-mediated disease encompassing ulcerative colitis (UC) and Crohn's disease (CD) [1,2]. IBD is hallmarked by excess immune cells in the gastrointestinal tract and complex inflammatory networks [3]. The innate immune system comprises macrophages, neutrophils, and dendritic cells [4–7]. Macrophages are intriguing targets for immune-mediated therapeutic strategies, specifically when there is a compromise in the barrier function of the gastrointestinal tract to induce aberrant inflammatory responses [8]. As well, macrophages play an important role in immune responses to pathogens and tolerance to commensals in the gut [9].

The T-cell immunoglobulin domain and mucin domain-3 (Tim-3, also known as HAVCR2) is a negative regulator of immune cells [10]. Tim-3 was first described as a marker of Th1 cells [10]; however, there is evidence that it is expressed in various immune cells, including Th17

* Corresponding author. Yongwai Street, Donghu District, Nanchang, Jiangxi Province, 330000, China
E-mail address: xieyong_med@ncu.edu.cn (Y. Xie).

https://doi.org/10.1016/j.redox.2024.103072
Received 5 January 2024; Received in revised form 27 January 2024; Accepted 31 January 2024
Available online 2 February 2024

cells [11], dendritic cells [12], natural killer (NK) cells [13], mast cells [14], and monocytes/macrophages [15]. The function of macrophage Tim-3 in intestinal inflammation remains unclear. UC is strongly linked to chronic inflammation, which may result from an aberrant immune response toward microbiota in the intestines and/or food antigens [16]. Macrophages, important antigen-presenting cells, play a central function in the pathogenesis of UC by presenting antigens to downstream adaptive immune cells [16,17]. Thus, we aimed to characterize the role as well as the mechanism of action of macrophage Tim-3 in patients with UC in this study.

Necroptosis, a recently identified cell death pathway that regulates intestinal homeostasis and inflammation, is a type of necrosis caused by death receptors, such as tumor necrosis factor (TNF)-α receptor 1, receptor-interacting protein kinase (RIP)1, and RIP3 [18]. These receptors activate the phosphorylation of mixed lineage kinase domain-like (MLKL) proteins, disrupting cell integrity [19]. A key component of necroptosis is the release of cellular contents, including potential damage-associated molecular patterns (DAMPs), such as high mobility group box 1 protein (HMGB1) and ATP [20,21]. The generation of Reactive Oxygen Species (ROS) has been suggested to contribute to necroptosis, although the sources and functions of ROS in this process are still not fully understood [22,23]. The dysregulation of necroptosis is important in inflammatory-based pathologies including IBD, sepsis, and neurodegenerative diseases [24]. Therefore, inhibition of necroptosis is a potentially effective treatment strategy for myriad diseases involving inflammation and cell death [25]. However, the role of necroptosis in IBD pathogenesis remains elusive.

Neutrophils, the most abundant immune cell type, constitute the first line of immune defenses [26]. However, excessive recruitment of neutrophils results in tissue damage in IBD [27]. Specifically, neutrophils promote gut inflammation in IBD by secreting high levels of reactive oxygen species (ROS), which disrupt the epithelial barrier and enhance redox-sensitive inflammatory pathways [28]. Damage to the epithelial barrier can be attributed to the release of neutrophil-secreted proteases and pro-inflammatory cytokines, which recruit monocytes and neutrophils to the inflamed tissue [6]. Furthermore, tissue macrophages play an important role in neutrophil recruitment [29]; however, it remains unclear whether macrophages recruit neutrophils and subsequently induce neutrophil necroptosis.

This study characterizes the function and mechanism of action of macrophage Tim-3 in UC and shows that the Tim-3 expression level is remarkably elevated within the macrophages of patients with UC and the murine colitis model. Our findings underscore that macrophage Tim-3 acts as a determinant of neutrophil necroptosis and intestinal mucosal barrier, providing novel insights into UC treatment strategies.

2. Materials and methods

2.1. Human samples

Samples were extracted from CD or UC patients and healthy controls at The First Affiliated Hospital of Nanchang University (Nanchang, China). The Ethics Committee of the First Affiliated Hospital of Nanchang University approved this study [ethical approval number: (2022) CDYFYYLK(06-021)], and each participant provided informed consent. Colon samples were collected from patients undergoing colonoscopy or colon resection for IBD, or from healthy subjects undergoing colonoscopy surveillance. Mucosal biopsies from 48 patients with IBD (UC: 24 colon samples; CD: 24 ileum or colon samples) and 12 healthy volunteers were collected according to conventional protocols. Patient information is presented in Table S1. IBD was diagnosed by two experienced IBD-focused gastroenterologists through a routine diagnostic evaluation, utilizing the Porto criteria modified according to the ECCO guidelines [30].

2.2. Data collection

The NCBI GEO database provided both single-cell RNA sequencing (sc-RNA-seq) (GSE214695) and RNA array (GSE126124) data. First, the Seurat function "FindVariableFeatures" was employed to detect the highly variable genes (HVGs). Data integration involved utilizing the top 2000 HVGs. The information was rescaled using the "ScaleData" method, and the initial 40 principal components were selected for auto-clustering analysis through the "FindNeighbors" and "FindClusters" functions. Clusters were identified for every cell at a resolution of 1.5. A UMAP scatter plot was generated to visualize the cluster outcomes. The macrophage marker genes were obtained from the CellMark database.

2.3. Animal experiments

Both experimental and breeding mice were housed in a pathogen-free animal facility. All animal experiments were subjected to approval by the Animal Ethics Committee of Nanchang University (CDYFY-IACUC-202301QR046). C57BL/6 *Tim-3*$^{fl/fl}$ and Lys M-Cre mice were procured from Gempharmatech Co. Ltd. (Nanjing, China). *Tim-3* $^{fl/fl}$ mice were crossed with Lys M-Cre mice to obtain macrophage cell-specific *Tim-3*-knockout mice (LysMCre Tim-3 $^{fl/fl}$; Tim-3^{M-KO}).

2.4. Murine colitis models

To construct a murine colitis model, 3 % dextran sodium sulfate (DSS, MP Biomedicals) in drinking water was administered to wild-type (WT) C57BL/6 or Tim-3^{M-KO} mice for seven days, and the DSS water was changed every other day. On day 8, the animals were euthanized. The total body weight and survival rate were monitored. The clinical disease activity index (DAI) was assessed using clinical scores for stool type, weight loss, and bleeding, as previously described [31].

2.5. Histology

Mice were euthanized via CO_2 inhalation and tissue samples were collected and stored in RNAlater (M6101; New Cell & Molecular Biotech Co., Ltd; Suzhou, China). The rectal region of the colon was dissected, preserved in 4 % paraformaldehyde, and paraffinized. Hematoxylin and eosin-stained tissue sections were then examined under a light microscope (Optithot; Nikon). The histological scoring in our study was independently conducted by two pathologists.

2.6. Animal treatment

The following reagents were used in animal treatment: 5 mg/kg/day Nec-1 (HY-15760, MCE), 10 mg/kg/day GSK-872 (HY-101872, MCE), and 100 mg/kg/day NAC (HY–B0215, MCE). Drugs were dissolved as per the manufacturer's instructions. Control mice were intraperitoneally

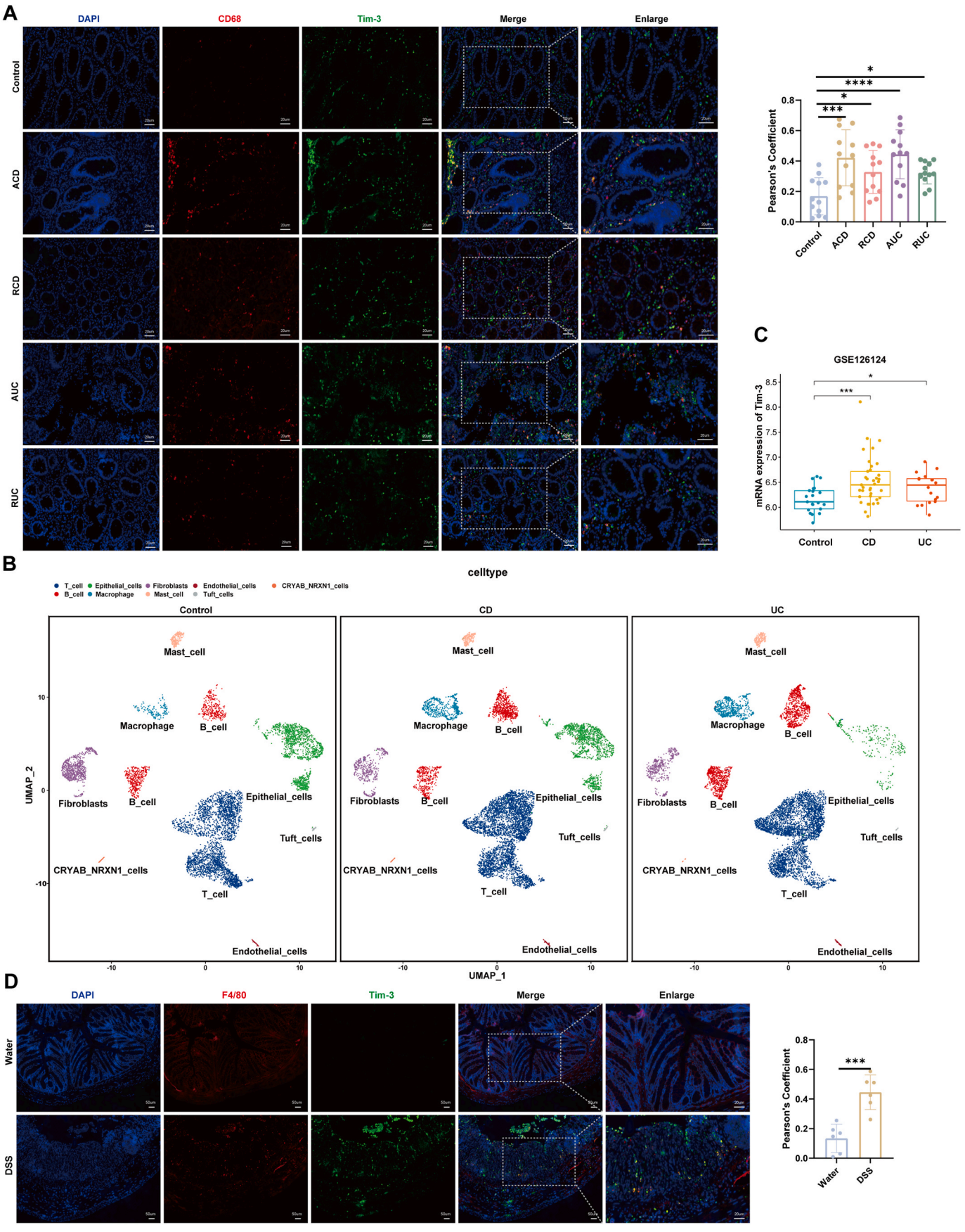

(caption on next page)

Fig. 1. Tim-3 expression level is elevated in the colonic macrophages of IBD tissues.
(A) Dual immunofluorescence staining for CD68 (red) and Tim-3 (green) in human colon biopsy tissues. The upper panel shows healthy tissues ($n = 12$), the middle panel shows active Crohn's disease (ACD) ($n = 12$) and CD in remission (RCD) tissues ($n = 12$), and the lower panel shows active ulcerative colitis (AUC) ($n = 12$) and UC in remission (RUC) tissues ($n = 12$). DAPI (blue)-stained nuclei. Scale bars: 20 μm. Quantitative analysis of CD68 colocalization with Tim-3 was carried out using the colocalization plugin of Image J. (B) UMAP findings illustrate the expression as well as distribution of Tim-3 in relation to single-cell clusters, accompanied by a box plot showcasing the levels of Tim-3 in colonocytes among patients with CD, UC, and healthy controls. $n = 6$ per group. (C) Quantification of Tim-3 expression in inflammatory bowel disease (IBD) patient datasets (GSE126124). The samples included healthy individuals ($n = 39$), and patients with CD ($n = 39$) and UC ($n = 18$), correspondingly. (D) Dual-immunofluorescence staining of F4/80 (red) and Tim-3 (green) in murine colon tissues. DAPI (blue)-stained nuclei. $n = 6$ for each group. Scale bars: 50 μm. Data are presented as the mean ± SD. $^{*}P < 0.05$, $^{***}P < 0.001$, $^{****}P < 0.0001$, in comparison to control group.

injected with a vehicle alone.

2.7. Cell culture and transfection

THP-1 and Caco2 cells were procured from Procell Life Science & Technology Co., Ltd. (Wuhan, China) and cultured in RPMI-1640 medium in a 5 % CO_2 atmosphere at 37 °C. THP-1 cells were transfected with lentivirus vectors (Tim-3-shRNA or control) following the manufacturer's specifications (Shanghai Jikai Gene, China). siRNAs as outlined below were utilized: 5′-GCCTTTCCAAGGATGCTTACC-3'; antisense: 5′-GGTAAGCATCCTTGGAAAGGC-3'. Following the lentiviral infection of THP-1 cells, stable shRNA-mediated knockdown cell lines were achieved by the selection of puromycin.

2.8. Reagents

Recombinant human TNF-α and IL-8 were purchased from PeproTech (PEPROTECH, NJ, USA). For the human TNF-α neutralization experiment, co-cultures were treated with 2 μg/ml anti-TNF-α mAb (Catalog no#SIM0001) or isotype mAb (human monoclonal IgG1) from Bio X cell (West Lebanon, NH). Human IL-8 neutralization mAb (2 μg/ml, Catalog no#MAB208) was obtained from R&D Systems. BAY11-7082 (Catalog no#S2913) and TAK-242 (Catalog no#S7455) were purchased from Selleck (Houston, TX, USA).

2.9. HL-60 cell differentiation model

The human promyelocytic leukemia cell line HL-60 was also procured from Procell Life Science & Technology Co., Ltd. (Wuhan, China) and cultured in IMDM (Iscove's modified Dulbecco's medium) in a humidified 5 % CO_2 incubator at 37 °C. An HL-60 cell density of 10^6 cells/ml underwent differentiation into neutrophil-like cells using 1.3 % DMSO for up to six days, as previously described [32].

2.10. Immunofluorescence/immunohistochemistry

For immunofluorescence staining, colonic sections measuring 4-μm were fixed using paraformaldehyde and permeabilized with Triton X-100 in phosphate-buffered saline, followed by subsequent blocking with blocking reagents. Next, the tissues were incubated with the appropriate primary antibodies and thereafter with a FITC-conjugated secondary antibody (Abcom, England). Staining intensity was determined using Image J. Colocalization studies were analyzed by Image J Just Another Colocalization Plugin (JACoP) (US National Institutes of Health), which provided Pearson's correlation coefficient (r) as a means to measure the degree of colocalization of objects in dual-color images. Immunohistochemistry was performed on mice colon tissue as described previously [33]. Table S2 lists primary antibodies.

2.11. RNA extraction and quantitative qRT-PCR

RNA from animal tissues or cultured cells was extracted using an RNA Extraction Kit (19221 ES; Yeasen Biotechnology, Shanghai, China) as per the manufacturer's instructions. Total RNA was subjected to reverse transcription using a Reverse Transcription kit (11184ES08; Yeasen Biotechnology). Quantitative PCR was performed utilizing the Hieff® qPCR SYBR Green Master Mix (11184ES08; Vazyme Biotechnology, Nanjing, China). All primer sequences are listed in Table S3.

2.12. Western blot analysis

The RIPA lysis buffer (R0020, Solarbio, Beijing, China) was used to homogenize the colonic samples, and the concentration of the total protein was measured. Primary antibodies are listed in Table S2. Immunoblots were displayed using an ECL detection kit (Thermo Fisher, USA), and the ChemiDoc MP System (Bio-Rad) was used to expose the blots digitally. The results were normalized using β-actin as an internal control. Full-length scans of immunoblots with key data are shown in Supplementary Fig. S4.

2.13. RNA-seq

RNA-seq was performed by OEBiotech (Shanghai, China). To prepare the cDNA library for RNA-seq, total RNA was isolated from the colonic tissues of WT and Tim-3^{M-KO} mice using an RNA Extraction Kit. An Agilent Technologies 2100 Bioanalyzer (Agilent Technologies) played a primary role in assessing the integrity of the RNA. The Illumina HiSeq 2500 platform was used to perform RNA-seq, and the Qubit 2.0 Fluorometer (Invitrogen) was used to visualize the RNA-seq data. Fold changes >2 and $P < 0.05$ denoted differentially expressed genes (DEGs).

3. ELISA

The secreted cytokines in the supernatants from the cell cultures were screened using a human cytokine ELISA plate array (Sangon Biotech, Shanghai, China) as per the manufacturer's instructions.

3.1. ROS measurement

ROS generation was assessed using the ROS detection kit (Thermo Fisher, USA) following the manufacturer's specifications. Semi-quantification of ROS levels was evaluated using ImageJ software.

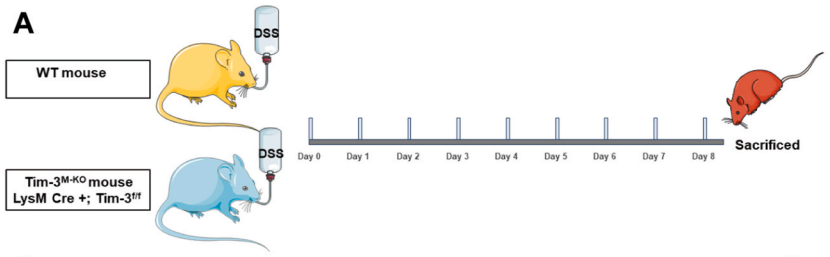

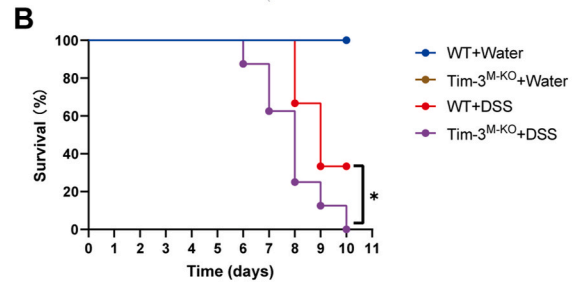

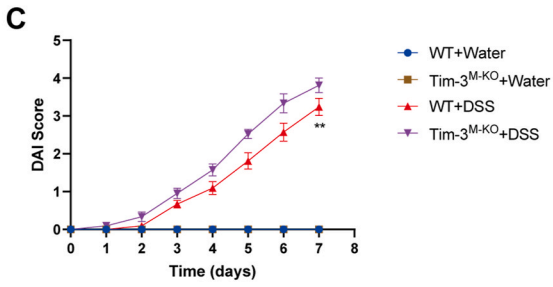

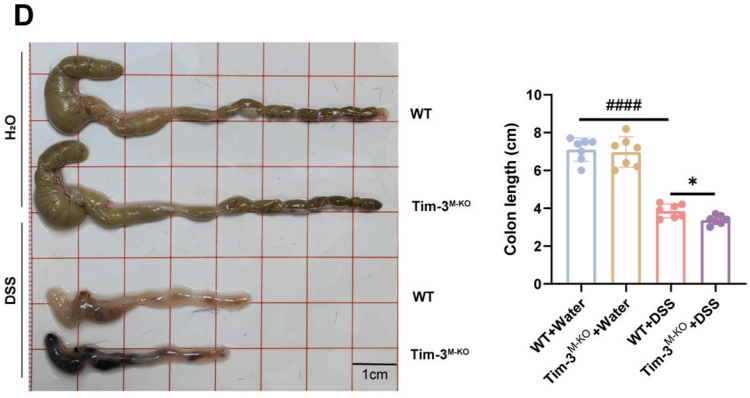

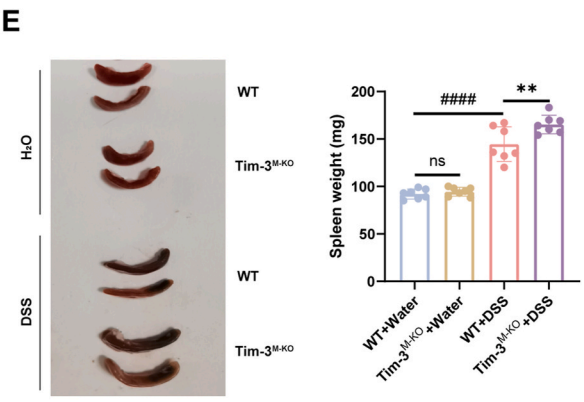

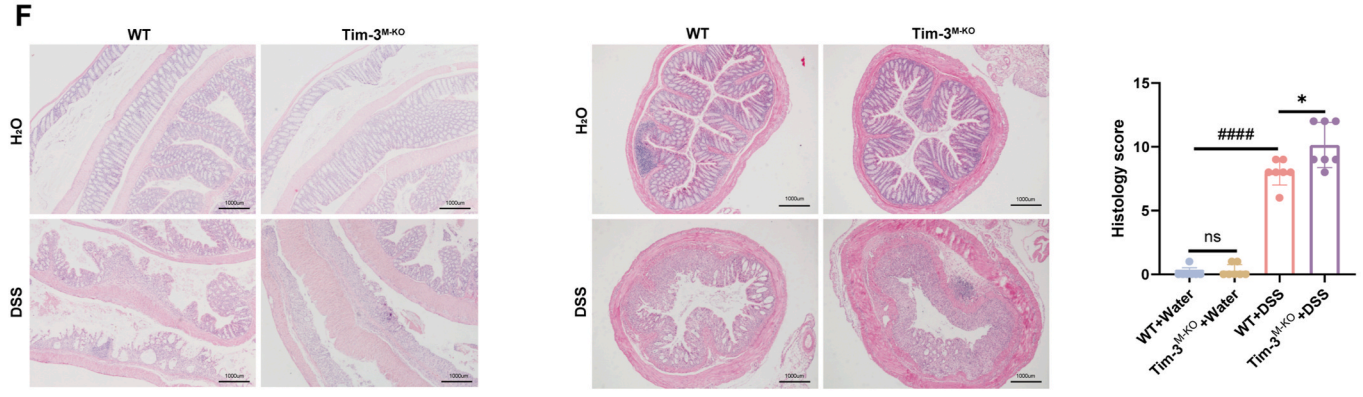

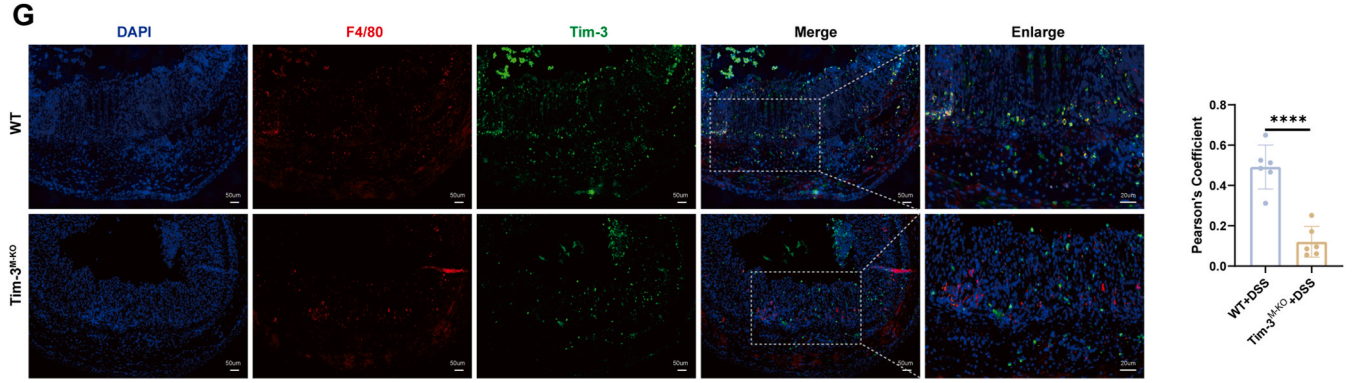

(caption on next page)

Fig. 2. Tim-3 in macrophages protects mice from acute colitis.
(A) Summary of the experimental protocol for experimental colitis in wild-type (WT) and macrophage-specific Tim-3 deletion (Tim-3^{M-KO}) mice. (B) WT and Tim-3^{M-KO} mice's relative survival rate. $n = 7$ for each group. The survival curve was generated utilizing the Kaplan-Meier approach and compared using the log-rank test. (C–F) WT and Tim-3^{M-KO} mice were fed with 3 % DSS for 7 days. $n = 7$ mice per group. (C) The mouse disease activity index (DAI) was documented daily. (D) The colony length and (E) spleen weight of each mouse was evaluated. Representative pictures were taken on day 8. (F) An H&E staining representative diagram of the entire colonic intestine and colon cross-sections. Histological analysis of the colon tissue. Scale bars: 1000 μm. (G) Immunofluorescence staining confirming successful knockdown of Tim-3 in macrophages. $n = 6$ mice per group. Scale bars: 50 μm. Data are presented as mean ± SD except those in Fig. 2C, which were presented as mean ± SEM. $^{*}P < 0.05$, $^{**}P < 0.01$, $^{****}P < 0.0001$ versus WT colitis mice; ####$P < 0.0001$ versus WT control mice; ns, no significance.

3.2. Neutrophil migration assay

Transwell migration assay (4.0 μm pore size, 24-well plate, Corning Inc., Corning, USA) was used for neutrophil migration assays. To prepare the supernatant for placement in the lower chamber, THP-1 cells (~2×10^5 cells/well) were treated with phorbol 12-myristate 13-acetate (PMA; 100 ng/ml) for 48 h. PMA-differentiated THP-1 cells were stimulated with 400 ng/ml lipopolysaccharide (LPS) for 6 h. A culture of differentiated HL-60 cells was incubated in serum-free RPMI-1640 medium in the upper chamber for 24 h. Incubation was followed by staining and analysis of the cells that had migrated to the lower chamber. The number of migrated neutrophils was evaluated by ImageJ.

3.3. Isolation of peripheral blood neutrophils

Primary neutrophils were extracted from the peripheral blood of C57BL/6J mice. The neutrophils were isolated using a mouse neutrophil isolation kit (P9201; Solarbio, Beijing, China) as per the manufacturer's protocols.

3.4. Phalloidin F-actin staining

Actin filaments were stained using Alexa Fluor 488-conjugated phalloidin (Invitrogen, Carlsbad, CA USA). Phalloidin-stabilized microfilaments were captured under a fluorescence microscope (Optithot, Nikon).

3.5. Statistical analysis

Two groups were compared using Student's *t*-tests. One-way analysis of variance (ANOVA) was performed to compare more than two groups. The survival curve was analyzed using the Kaplan-Meier method. GraphPad Prism 8.0 and SPSS 12.0 were used to perform all statistical analyses.

4. Results

4.1. Tim-3 expression is upregulated in the colonic macrophages of IBD tissues

First, we evaluated the role of macrophage Tim-3 in IBD pathogenesis by measuring its levels in the colonic mucosa of IBD patients. Dual immunofluorescence staining affirmed that macrophage Tim-3 was expressed at higher levels in patients with IBD that had inflamed colonic mucosa than in healthy controls (Fig. 1A). Moreover, tissue expression of macrophage Tim-3 positively correlated with disease severity. To validate the increase in Tim-3 expression in human macrophages, we utilized a single-cell RNA sequencing dataset of colonic tissues from a combined healthy, UC, and CD cohort (Fig. S1A). UMAP plots showed differential distribution and apparent differences in Tim-3 expression in these cell clusters: Tim-3 expression was upregulated in the macrophages of IBD patients versus controls (Fig. 1B and Fig. S1B). Moreover, Gene Expression Omnibus (GEO) datasets showed significant increases in Tim-3 mRNA levels in IBD samples compared to healthy individuals (Fig. 1C).

To corroborate these findings, we evaluated Tim-3 expression in DSS-induced colitis mice. Dual immunofluorescence staining showed that the number of Tim-3 positive macrophages was remarkably elevated in colitis colon samples than in controls (Fig. 1D). Collectively, these findings demonstrate that Tim-3 expression in macrophages is significantly augmented in the colonic tissues impacted by colitis.

4.2. Tim-3 in macrophages protects mice from DSS-induced colitis

Next, we crossed *Tim-3*$^{fl/fl}$ mice with Lys M-Cre mice to generate macrophage-specific *Tim-3*-deficient (Tim-3^{M-KO}) mice. The DSS was utilized to induce colitis in WT as well as Tim-3^{M-KO} mice (Fig. 2A). We first challenged WT and Tim-3^{M-KO} mice with 4 % DSS in drinking water to determine the survival rates. Tim-3^{M-KO} mice had a significantly diminished survival rate compared with control mice, which affirms that macrophage Tim-3 plays a protective function in colitis (Fig. 2B). Moreover, to generate an experimental colitis model, mice were administered 3 % DSS in drinking water. Tim-3^{M-KO} mice exhibited higher disease activity than DSS-treated WT mice (Fig. 2C). Consistent with clinical scores, Tim-3^{M-KO} mice also displayed shorter colons and moderate splenomegaly (Fig. 2D and E). The colons of Tim-3^{M-KO} mice also exhibited inflammatory features, such as inflammation severity, ulceration/erosion extension, and crypt disarray (Fig. 2F). Immunofluorescence staining was used to assess the knockdown efficiency of Tim-3 in macrophages. A significant decrease in Tim-3 expression was observed in the colonic macrophages from Tim-3^{M-KO} mice (Fig. 2G), confirming successful knockout. These data suggest that Tim-3 is induced in macrophages in response to DSS colitis and protects against intestinal damage.

4.3. Macrophage Tim-3 deficiency aggravates inflammation and M1 polarization in the colon

As Tim-3^{M-KO} mice exhibit marked colitis, we examined the expression of inflammatory molecules. qRT-PCR analysis revealed a significant increase of proinflammatory mediators (TNF-α, IL-1β, and IL-6) and chemokines (CCL2, CCL3, CCL4, CXCL1, and CXCL2) in DSS-treated Tim-3^{M-KO} mice (Fig. 3A). We next quantified M1 macrophages in colonic slices and found that CD86 and iNOS staining was significantly stronger in the colonic tissue of Tim-3^{M-KO} mice (Fig. 3C and D). Macrophage Tim-3 deficiency could enhance the polarization of

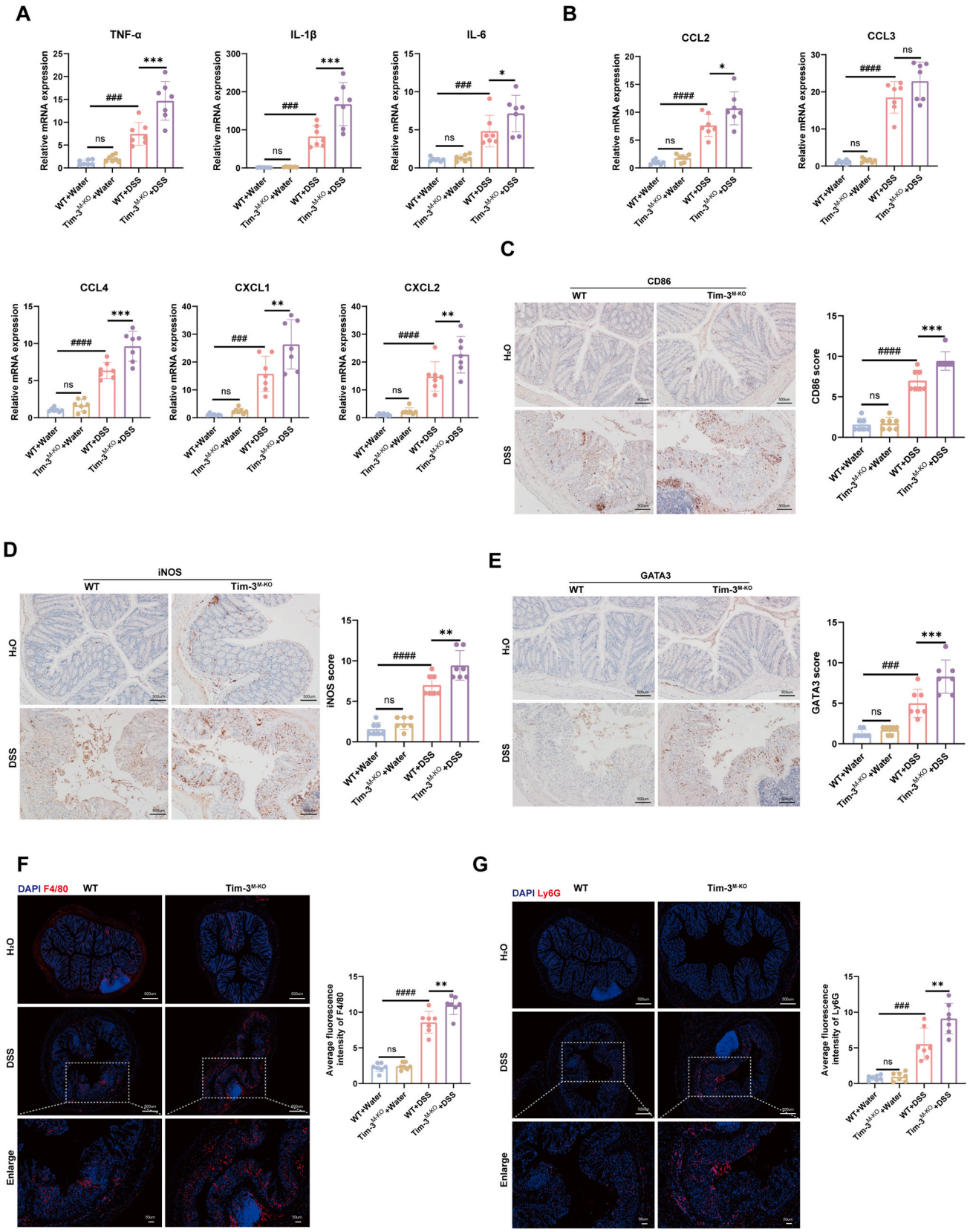

Fig. 3. Macrophage Tim-3 deficiency aggravates inflammation and M1 polarization in the colon.
(A, B) qRT-PCR examination of proinflammatory molecule expression in mouse colonic tissue isolated from WT and Tim-3^{M-KO} mice with or without DSS treatment. $n = 7$ mice per group. (C–E) Immunohistochemical staining of M1 macrophage markers (CD86 and iNOS) and Th2 cell marker (GATA3) in colonic tissues. $n = 7$ mice per group. Scale bars: 500 μm. (F–G) Immunofluorescence staining of F4/80 and Ly6G in colon tissues ($n = 7$). Scale bars: 500 μm. Data are presented as the mean ± SD. $^{*}P < 0.05$, $^{**}P < 0.01$, $^{***}P < 0.001$ versus WT colitis mice; $^{\#\#\#}P < 0.001$, $^{\#\#\#\#}P < 0.0001$ versus WT control mice; ns, no significance.

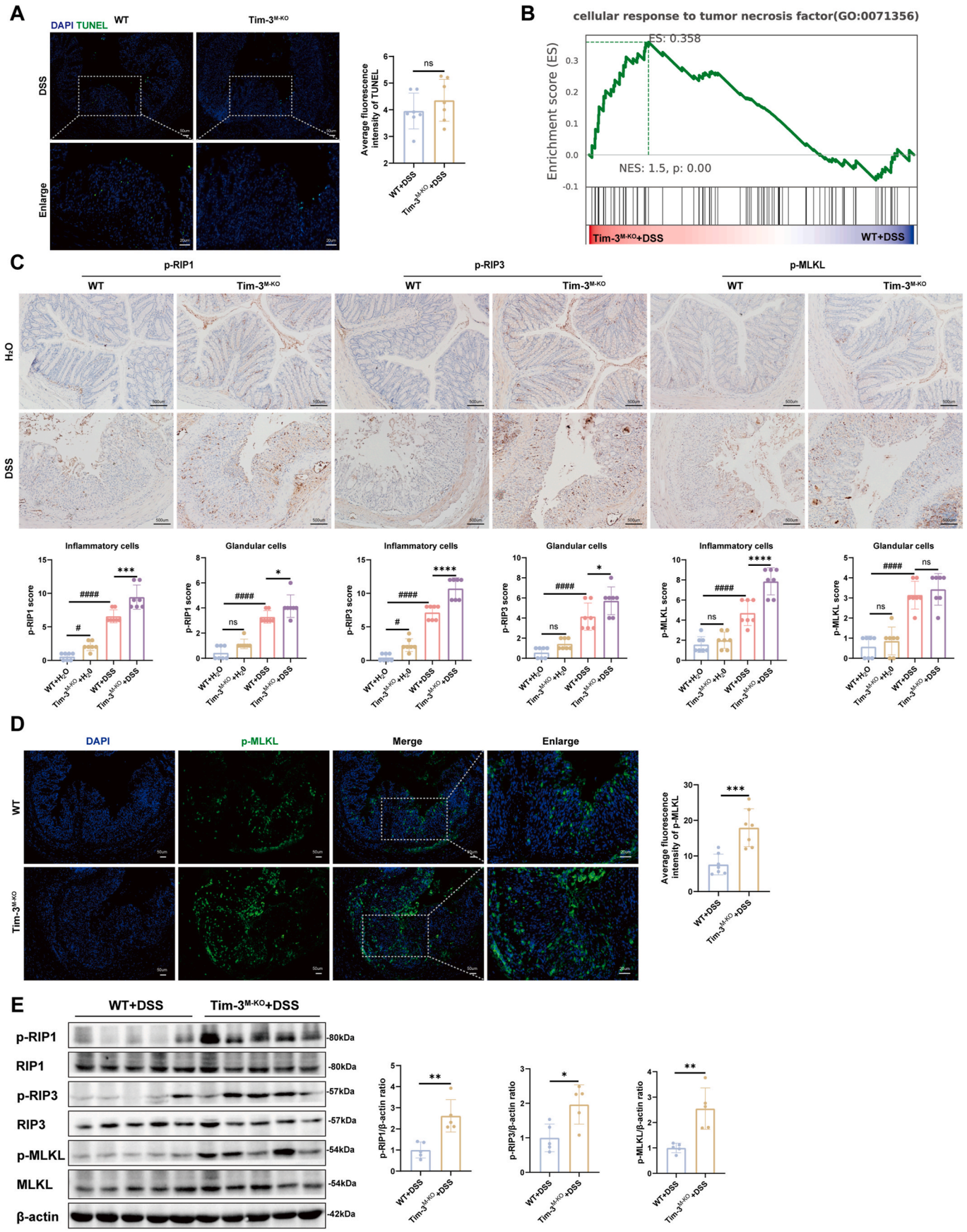

(caption on next page)

Fig. 4. Macrophage Tim-3 deficiency promotes necroptosis.
(A) TUNEL staining representative images (green, TUNEL-positive staining; blue, DAPI). $n = 7$ mice per group. Scale bars: 50 μm. (B) Gene Set Enrichment Analysis (GSEA) of colonic differentially expressed genes (DEGs) between DSS-treated WT and Tim-3^{M-KO} mice using RNA-seq analysis (n = 3). GSEA suggested significant enrichment of the cellular response to tumor necrosis factor pathway ($n = 3$). (C) Immunohistochemical staining of p-RIP1, p-RIP3, and *p*-MLKL in colonic tissues. Quantification of the relative number of positive cells is shown in the graph below ($n = 7$). Scale bars: 500 μm. (D) Immunofluorescence staining of *p*-MLKL in the colonic tissues ($n = 7$). Scale bars: 50 μm. (E) Western blot analysis of p-RIP1, p-RIP3, and *p*-MLKL protein levels, and quantitative analyses were performed using ImageJ ($n = 5$ for each group). Data are presented as the mean ± SD. $^{*}P < 0.05$, $^{**}P < 0.01$, $^{***}P < 0.001$, $^{****}P < 0.0001$ versus WT colitis mice; $\#P < 0.05$, $\#\#\#\#P < 0.0001$ versus WT control mice; ns, no significance.

macrophages toward a pro-inflammatory M1 phenotype. Furthermore, Th2 cells have been previously identified as the dominant T helper cell subset involved in UC [34]. Fig. 3E shows that Tim-3^{M-KO} mice exhibited increased GATA3—a key transcriptional regulator in Th2 cells—expression compared with control colons. These results suggest that macrophage Tim-3 deficiency alters intestinal macrophage subsets and adaptive immune T cell populations during colitis. We also examined the accumulation of colonic inflammatory cells using F4/80 (macrophage marker) and Ly6G (neutrophil marker) staining in colonic tissues. In comparison to WT mice, macrophage Tim-3 deficiency substantially enhances macrophages as well as neutrophils infiltration in the colon during colitis (Fig. 3F and G).

4.4. Macrophage Tim-3 deficiency promotes necroptosis

To ascertain if macrophage Tim-3 deficiency is involved in apoptosis during colitis, we quantified the number of apoptotic events in the colon of WT and Tim-3^{M-KO} mice. However, there was no significant variation between the groups in the number of TUNEL-positive cells (Fig. 4A). The result excluded a significant contribution of apoptosis in this model. To further study macrophage Tim-3 deficiency induced molecular changes, we conducted an RNA-Seq analysis. Gene Set Enrichment Analysis (GSEA) revealed that the cellular response to tumor necrosis factor pathway was significantly enriched in DSS-treated Tim-3^{M-KO} mice (Fig. 4B). Tumor necrosis factor triggers necroptosis in response to tissue injury and inflammation [35]. RIP1, RIP3, and MLKL are key factors that trigger necroptosis, and their activation generally involves phosphorylation and translocation to the membrane [36]. When *p*-MLKL oligomers translocate to the cell membrane, the intracellular osmotic pressure increases, leading to membrane rupture [37]. Therefore, we examined necroptosis in the colon via immunohistochemistry and immunofluorescence. DSS-treated Tim-3^{M-KO} mice upregulated the expression of p-RIP1, p-RIP3, and *p*-MLKL (Fig. 4C). Tim-3^{M-KO} mice also showed a greater propensity to translocate *p*-MLKL from the cytoplasm to the plasma membrane (Fig. 4D). This result was confirmed via Western blot analysis of core necroptosis-related factors (Fig. 4E). Collectively, the results indicate that macrophage-specific Tim-3 deficiency induces intestinal necroptosis.

4.5. Pharmacological inhibition of RIP1 or RIP3 alleviates colitis in Tim-3^{M-KO} mice

Tim-3 ablation in macrophages contributes to aggravated colitis due to excessive necroptosis. Nec-1 (a RIP1 kinase activity-related chemical inhibitor) and GSK-872 (a chemical inhibitor of RIP3 kinase activity) are potent and specific necroptosis inhibitors and were, therefore, used to assess whether necroptosis actively contributes to excessive colitis (Fig. 5A). The colitis was attenuated in Tim-3^{M-KO} mice treated with Nec-1 or GSK-872 (Fig. S2A). The Tim-3^{M-KO} mice treated with drugs also showed histological recovery with less epithelial damage less inflammatory infiltration, and increased colon length (Fig. 5B and Fig. S2B). Daily treatment consistently reduced neutrophil infiltration and cytokine production (Fig. 5C and Fig. S2C). In addition, Nec-1 or GSK-872 treatment substantially attenuated DSS-induced phosphorylation of RIP1, RIP3, and MLKL in Tim-3^{M-KO} mice (Fig. 5D). Together, these data affirm that necroptosis activation contributes to excessive colitis in Tim-3^{M-KO} mice.

4.6. Tim-3 deficient macrophages increase neutrophil necroptosis

The histopathological feature predominant in IBD is the infiltration of acute and chronic inflammatory cells, including macrophages, neutrophils, and T cells [38–42]. We found that p-RIP1, p-RIP3, and *p*-MLKL levels in inflammatory cells were higher than those in glandular cells (Fig. 4C). A significant decrease in p-RIP1/p-RIP3/p-MLKL in inflammatory cells was observed in Tim-3^{M-KO} mice administered with Nec-1 or GSK-872 (Fig. 5D). Double-immunofluorescence staining for *p*-MLKL, and F4/80, Ly6G or CD3, confirmed that *p*-MLKL was expressed predominantly by $Ly6G^{+}$ neutrophils after Tim-3 knockdown in macrophages (Fig. 6A, B and C). Thus, we postulated that Tim-3 deficient macrophages increase neutrophil necroptosis.

Previous reports have indicated that macrophages recruit neutrophils by secreting chemokines [29]. IL-8 acts as a chemoattractant for neutrophils during inflammation [43,44]. Meanwhile, the expression of CXCR1 and/or CXCR2 on neutrophil surfaces is directly linked to neutrophil migration [29]. Therefore, we examined IL-8, CXCR1, and CXCR2 expression in mouse colonic mucosa. The inflammatory cytokines were upregulated in Tim-3^{M-KO} mice treated with DSS (Fig. 6D). Moreover, the expression of myeloperoxidase (MPO)—an antimicrobial enzyme that is expressed abundantly in neutrophils—was higher in Tim-3^{M-KO} mice than in WT colonic tissues (Fig. 6E), indicating the increased presence or activation of neutrophils in Tim-3^{M-KO} mice. This result suggests that Tim-3^{M-KO} mice had a greatly increased propensity to develop colitis compared with their WT mice. GSEA also supports the functional role of the neutrophil chemotaxis pathway (Fig. 6F). Therefore, based on the results of this study and those of previous studies, we speculate that neutrophils are recruited to inflammatory sites by chemokines released from Tim-3 knockdown macrophages and further trigger necroptosis.

4.7. Tim-3 deficient macrophages induce neutrophil chemotaxis and trigger necroptosis

To better understand how Tim-3 deficient macrophage-neutrophil

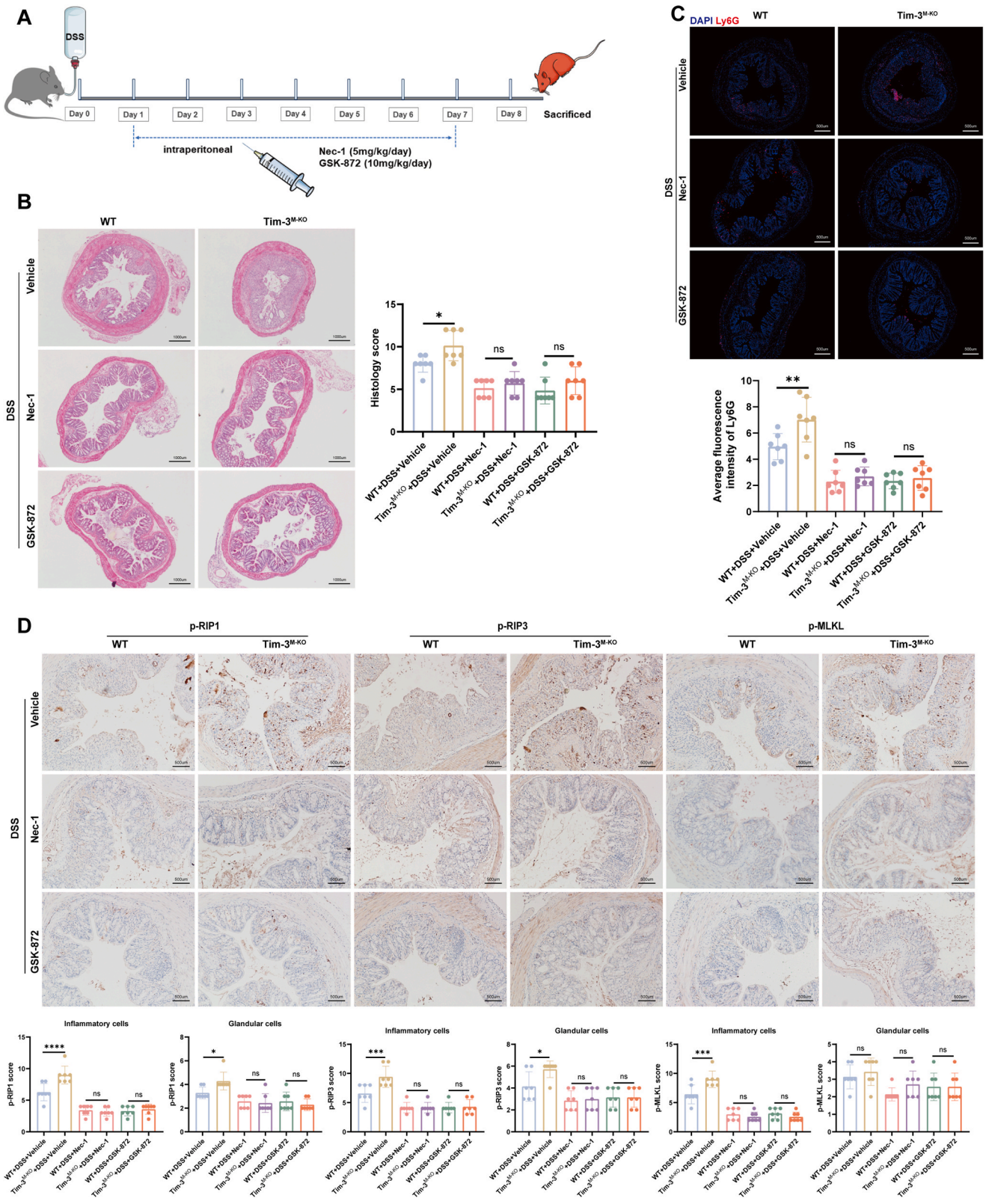

Fig. 5. Pharmacological inhibition of RIP1 or RIP3 alleviates colitis in macrophage Tim-3 deficient mice.
(A) An illustration of the study design. Mice were intraperitoneally treated with either the vehicle control, Nec-1 (5 mg/kg/day), or GSK-872 (10 mg/kg/day) throughout the entire experimental period. $n = 7$ mice per group. (B) H&E staining representative diagram of colon cross-sections. Histological analysis of the colon tissue. Scale bars: 1000 μm. $n = 7$ mice per group. (C) Immunofluorescence staining of Ly6G in colon tissues ($n = 7$). Scale bars: 500 μm. (D) Immunohistochemical staining of p-RIP1, p-RIP3, and *p*-MLKL in colonic tissues from DSS-treated mice with or without Nec-1 or GSK-872 administration on day 7. The quantification of the relative number of positive cells is shown in the graph below ($n = 7$). Scale bars: 500 μm. Data are presented as the mean ± SD. $^{*}P < 0.05$, $^{**}P < 0.01$, $^{***}P < 0.001$, $^{****}P < 0.0001$ versus WT colitis mice; ns, no significance versus WT colitis mice treated with pharmacological inhibitors.

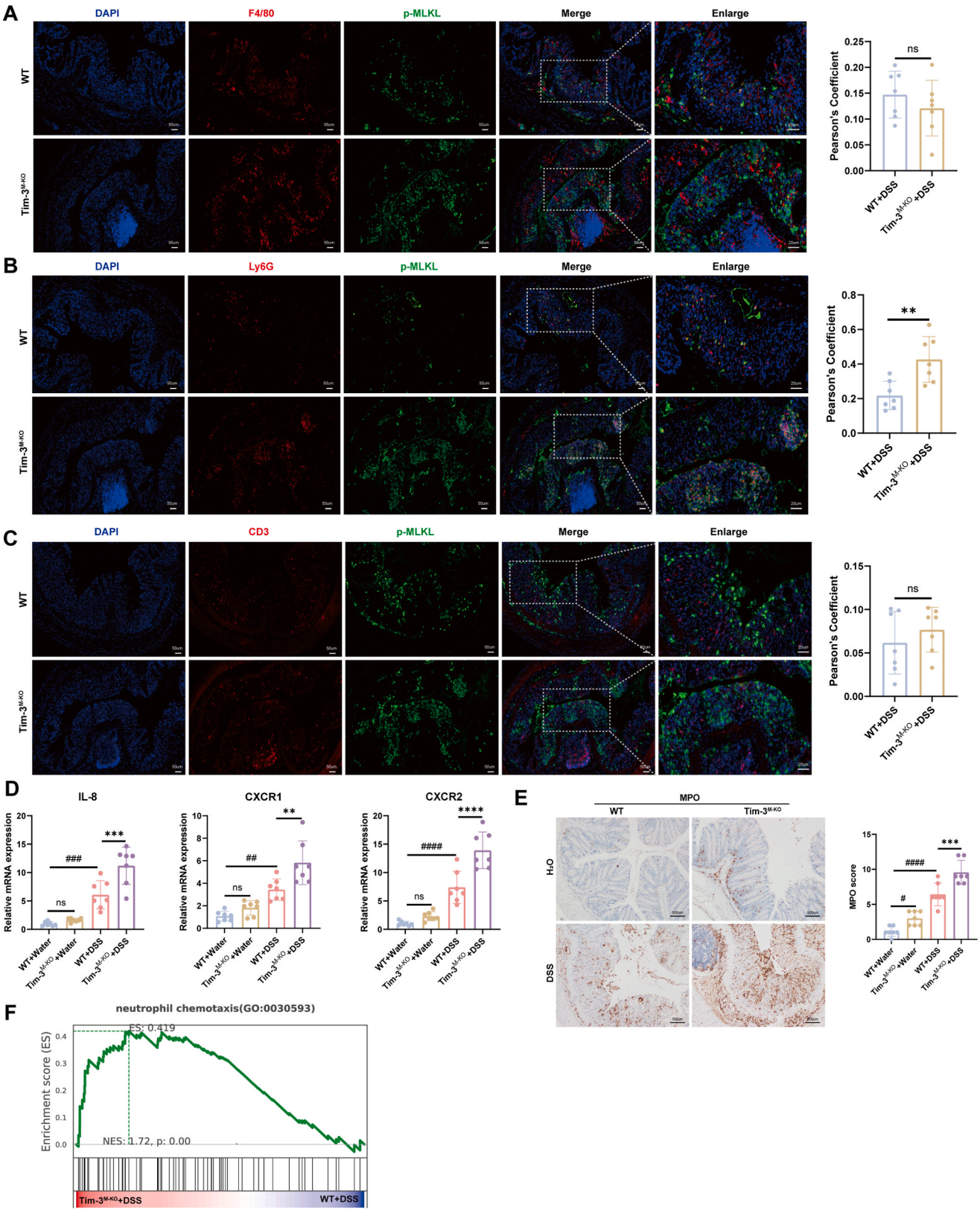

Fig. 6. Tim-3 deficient macrophages increase neutrophil necroptosis.
(A) Dual-label immunofluorescence of colonic tissues of WT and Tim-3^{M-KO} mice using F4/80 (red) and *p*-MLKL (green) antibodies ($n = 7$). Scale bars: 50 μm. (B) Dual-label immunofluorescence for Ly6G (red) and *p*-MLKL (green) ($n = 7$). Scale bars: 50 μm. (C) Dual-label immunofluorescence for CD3 (red) and *p*-MLKL (green) ($n = 7$). Scale bars: 50 μm. (D) qRT-PCR analysis of IL8, CXCR1, and CXCR2 expression in the colons of WT and Tim-3^{M-KO} mice. n = 7 mice per group. (E) Immunohistochemical staining of MPO in colon tissues of WT and Tim-3^{M-KO} mice. $n = 7$ mice per group. Scale bars: 500 μm. (F) GSEA analysis suggested substantial enrichment of the neutrophil chemotaxis pathway ($n = 3$). Data are presented as the mean ± SD. $^{**}P < 0.01$, $^{***}P < 0.001$, $^{****}P < 0.0001$, versus WT colitis mice; ns, no significance; $\#\#P < 0.01$, $\#\#\#P < 0.001$, $\#\#\#\#P < 0.0001$, versus WT control mice.

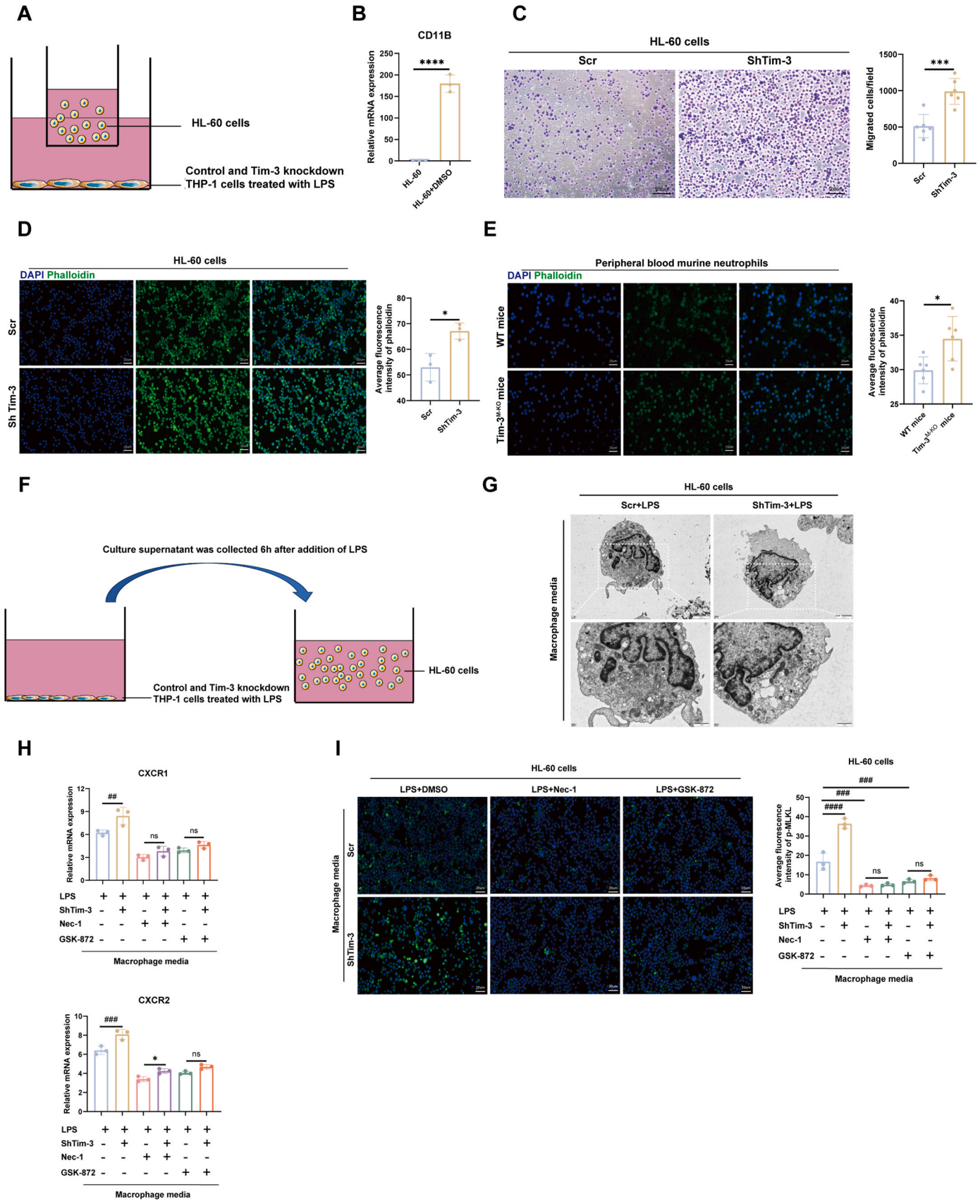

(caption on next page)

Fig. 7. Tim-3 deficient macrophages induce neutrophil chemotaxis and trigger necroptosis.
(A) Schematic of *in vitro* co-culture experiments. (B) qRT-PCR analysis of CD11B mRNA in DMSO-treated HL-60 cells (n = 3). (C) Neutrophil migration with crystal violet induced by control (Scr) and Tim-3 knockdown (ShTim-3) THP-1 cells (n = 6 for each group). Scale bars: 500 μm. (D) Phalloidin staining of the actin cytoskeleton in HL-60 cells. HL-60 cells were co-cultured directly with Scr or ShTim-3 THP-1 cells. The bar charts show the average fluorescence intensity of phalloidin (n = 3 for each group). Scale bars: 20 μm. (E) Phalloidin staining of the actin cytoskeleton in peripheral blood of murine neutrophils. Peripheral blood neutrophils were collected from WT and Tim-3^{M-KO} mice on day 8 following DSS administration. The bar charts show the average fluorescence intensity of phalloidin (n = 6 for each group). Scale bars: 20 μm. (F) Study design. THP-1 cells were incubated with LPS. The supernatant of Scr or ShTim-3 THP-1 cells was harvested and added to HL-60 cells. The HL-60 cells underwent pretreatment with the RIP1 inhibitor (30 μM Nec-1) or RIP3 inhibitor (50 μM GSK-872) for 30 min (n = 3). (G) TEM images showing the typical morphology of necroptosis in HL-60 cells treated with the supernatant from Tim-3 knockdown macrophages. Scale bar, 2 μm (overview) and 1 μm (magnification). (H) qRT-PCR results of CXCR1 and CXCR2 in HL-60 cells. (I) Representative images of the immunofluorescence assay results for anti-*p*-MLKL (green) and DAPI (blue) staining, and quantitative analyses were performed using ImageJ (n = 3). Data are presented as the mean ± SD. $^{*}P < 0.05$, $^{***}P < 0.001$, $^{****}P < 0.0001$; $\#\#P < 0.01$, $\#\#\#P < 0.001$, $\#\#\#\#P < 0.0001$; ns, no significance.

interactions occur, we performed a coculture experiment (Fig. 7A). HL-60 cells were exposed to DMSO for six days to differentiate into neutrophil-like cells [45]. As indicated by the increased CD11b expression, DMSO treatment induced HL-60 differentiation (Fig. 7B). THP-1 cells were subjected to differentiation into macrophages via PMA and cultured with LPS to simulate *in vivo* inflammatory microenvironment in patients with UC. Transwell assays revealed that Tim-3 knockdown (ShTim-3) macrophages enhanced the migration of HL-60 cells compared to negative control cells (Fig. 7C). Phalloidin staining showed that Tim-3 knockdown-induced F-actin polymerization in HL-60 cells (Fig. 7D). Since HL-60 cells are a transformed cell line, we repeated the experiment with peripheral blood murine neutrophils. WT and Tim-3^{M-KO} mouse whole blood were collected after 7 days of DSS treatment. Peripheral blood neutrophils stained with phalloidin yielded similar results (Fig. 7E).

To further explain the macrophage-neutrophil interaction mechanisms, the LPS-treated THP-1 cell culture supernatant was collected and added to HL-60 cell cultures (Fig. 7F). Following stimulation for 4 h, HL-60 cells were harvested for transmission electron microscopy (TEM) analyses. TEM images revealed exacerbated subcellular features of necrosis-like swelling and plasma membrane discontinuation of HL-60 cells treated with the supernatant from Tim-3 knockdown macrophages (Fig. 7G). HL-60 cells pretreated in the presence or absence of Nec-1 or GSK-872 were also collected for qRT-PCR assay. HL-60 cells treated with the supernatant from Tim-3 knockdown macrophages exhibited significantly increased CXCR1 and CXCR2 expression compared with the negative control; the RIP1 or RIP3 inhibitor significantly downregulated their expression (Fig. 7H). The HL-60 cells were also harvested for immunofluorescence. HL-60 cells treated with culture supernatant from Tim-3 knockdown macrophages produced more *p*-MLKL protein compared with the negative control (Fig. 7I). Following treatment with Nec-1 or GSK-872, no substantial differences were observed between groups.

To further confirm the role of the macrophage-secreted factor(s), the cell supernatant of macrophages was extracted, and ELISA was performed to study the paracrine effect. TNF-α is the classical initiator of necroptosis through TNF-α/RIP1/RIP3/MLKL signaling [19]. IL-8 is a chemotactic factor that guides the neutrophils to inflammation sites [44]. Significantly elevated TNF-α and IL-8 levels were observed in cell supernatants from Tim-3 knockdown macrophages (Fig. 8A). To determine whether neutrophil necroptosis is dependent on TNF-α and IL-8 secretion in Tim-3 knockdown macrophages, we antagonized TNF-α and IL-8 via the administration of neutralizing antibodies. Media from Tim-3 knockdown macrophages, induced neutrophil necroptosis, which was completely blocked by TNF-α antibodies (Fig. 8B). This indicates a direct effect of TNF-α on neutrophil necroptosis. We next assessed whether Tim-3 knockdown macrophages induce neutrophils chemotaxis via activation of the IL-8. As expected, the neutralizing IL-8 antibodies inhibited the chemotaxis of neutrophils co-cultured with Tim-3 knockdown macrophages (Fig. 8C). To further confirm the role of TNF-α in neutrophil necroptosis, we treated HL-60 cells with recombinant human TNF-α. The p-RIP1, p-RIP3, and *p*-MLKL protein expression increased with increasing TNF-α concentrations in a concentration-dependent manner (Fig. 8D). HL-60 cells treated with recombinant human TNF-α produced more *p*-MLKL protein compared with the negative control (Fig. 8E). Following treatment with Nec-1 or GSK-872, no substantial differences were observed between groups. To test this hypothesis, we analyzed the TNF-α and IL-8 expression level on macrophages in the Tim-3^{M-KO} mice. Double-immunofluorescence staining for F4/80, and TNF-α or IL-8, confirmed that TNF-α and IL-8 were expressed predominantly in Tim-3 knockdown macrophages (Fig. 8F and G). These results show that Tim-3 knockdown macrophages induce neutrophil chemotaxis via the release of IL-8 and trigger neutrophil necroptosis by TNF-α release.

4.8. Macrophage Tim-3 inhibits inflammatory responses via downregulating TLR4/NF-κB signaling pathway

We continued to explore the molecular mechanisms in Tim-3 knockdown macrophages. Tim-3 determines the severity of inflammation in mice in a TLR4-dependent manner [46–48]. The release of inflammatory cytokines and chemokines, such as IL-6, IL-8, TNF-α, and CCL2, is a widely recognized consequence of NF-κB activation [49,50]. We hypothesized that macrophage Tim-3 inhibits inflammatory responses via TLR4/NF-κB signaling pathway. Western blot analysis showed that the expression level of TLR4 and phosphorylation of p65 were significantly elevated in Tim-3 knockdown macrophages following LPS treatment (Fig. 9A). The findings from immunofluorescence staining with TLR4 and phosphorylation of p65 were consistent with those of the Western blot assay (Fig. 9B and C).

To further demonstrate that the TLR4/NF-κB signaling pathway is engaged by macrophage Tim-3, we made use of the TLR4-specific inhibitor TAK-242 and NF-κB-specific inhibitor BAY11-7082, respectively. As expected, the pro-inflammatory cytokines (TNF-α and IL-8) were downregulated in Tim-3 knockdown macrophages treated with inhibitors, further indicating that macrophage Tim-3 inhibited inflammation via the TLR4/NF-κB signaling pathway (Fig. 9D). The supernatants of each group were harvested and added to HL-60 cells. We

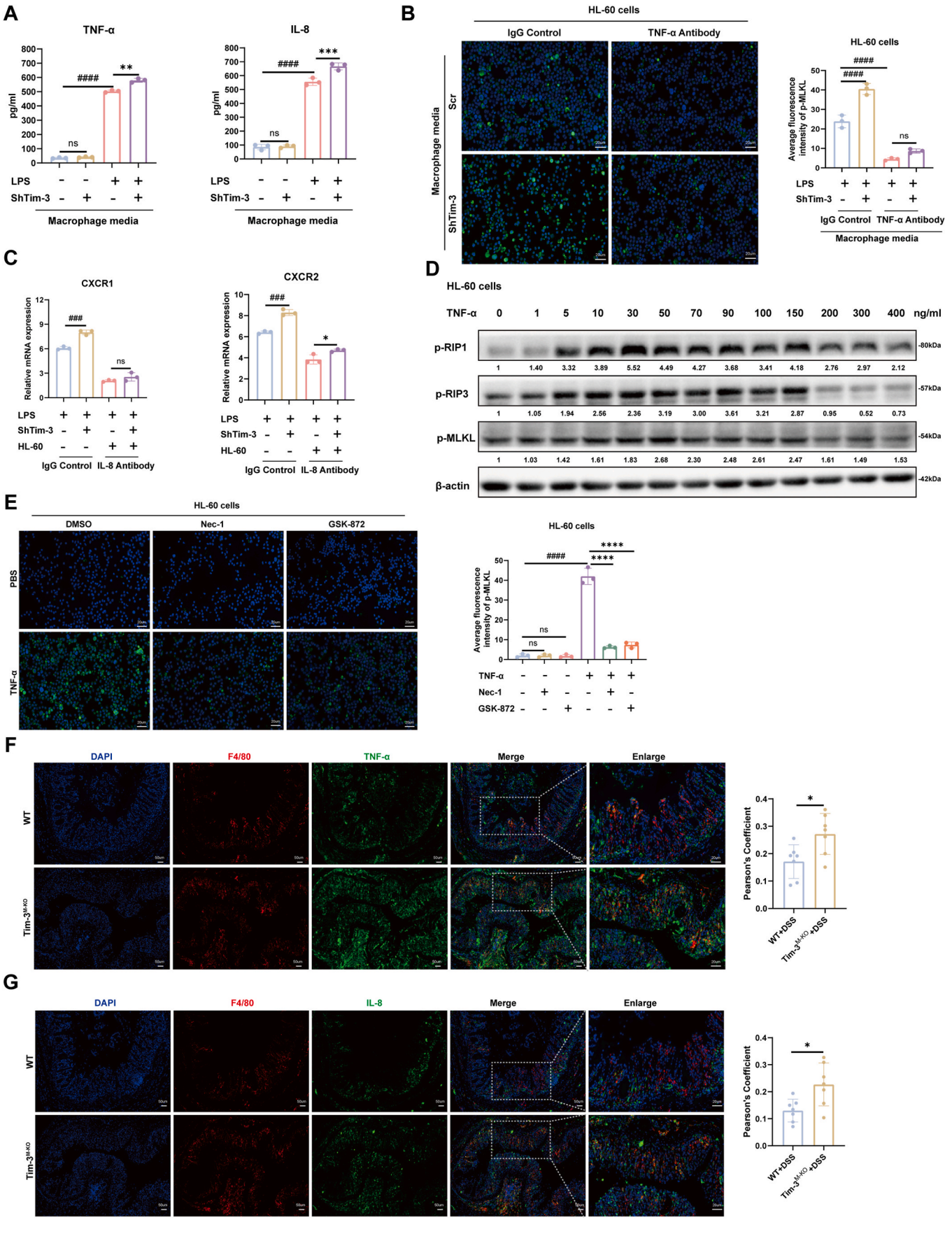

(caption on next page)

Fig. 8. Tim-3 deficient macrophages induce neutrophil chemotaxis via the release of IL-8 and trigger neutrophil necroptosis by TNF-α release.
(A) Control (Scr) and Tim-3 knockdown (ShTim-3) THP-1 cells were incubated for 6 h in medium alone or medium containing LPS (400 ng/ml); then the supernatants were tested for TNF-α and IL-8 (n = 3). (B) Representative images of *p*-MLKL^{+} immunofluorescent staining for HL-60 cells. THP-1 cells were incubated with LPS. The supernatant of Scr or ShTim-3 THP-1 cells underwent pretreatment with isotype control or anti-TNF-α antibody and added to HL-60 cells (n = 3). Scale bars: 20 μm. (C) qRT-PCR results of CXCR1 and CXCR2 in HL-60 cells. THP-1 cells were incubated with LPS. The supernatant of Scr or ShTim-3 THP-1 cells underwent pretreatment with isotype control or anti-IL-8 antibody and added to HL-60 cells (n = 3). (D) TNF-α-induced necroptosis upregulation is in a TNF-α dose-dependent manner. Necroptosis was stimulated with different doses of TNF-α as indicated. Protein was collected at 4 h after TNF-α stimulation (n = 3). (E) Representative images of *p*-MLKL^{+} immunofluorescent staining for HL-60 cells. The HL-60 cells underwent pretreatment with the RIP1 inhibitor (30 μM Nec-1) or RIP3 inhibitor (50 μM GSK-872) for 30 min. Then, HL-60 cells were incubated with TNF-α (50 ng/ml) or PBS (n = 3). Scale bars: 20 μm. (F) Dual-label immunofluorescence of colonic tissues of WT and Tim-3^{M-KO} mice using F4/80 (red) and TNF-α (green) antibodies (n = 7). Scale bars: 50 μm. (G) Dual-label immunofluorescence for Ly6G (red) and IL-8 (green) (n = 7). Scale bars: 50 μm. Data are presented as the mean ± SD. *$P < 0.05$, **$P < 0.01$, ***$P < 0.001$, ****$P < 0.0001$; ###$P < 0.001$, ####$P <$ 0.0001; ns, no significance.

stained HL-60 cells with phalloidin and found that the amount of rhodamine phalloidin-labeled F-actin was significantly decreased in the presence of both inhibitors (Fig. 9E). Moreover, both inhibitors abolished Tim-3 knockdown macrophages-induced necroptosis in neutrophils (Fig. 9F).

To clarify the effects of TLR4/NF-κB on Tim-3 knockdown macrophages in terms of functional properties, Scr or Tim-3 knockdown (ShTim-3) macrophages were seeded into the upper chamber of Transwell chambers; the results showed that TLR4 or NF-κB p65 inhibitor attenuates THP-1 Transwell migration capacity (Fig. 9G). Furthermore, Tim-3 ablation increased CCL2, CCL3, CCL4, CXCL1, and CXCL2 expression of macrophages when stimulated with LPS *in vitro*, consistent with the findings described in Fig. 3 (Fig. 9H). Both inhibitors completely blocked the upregulation of the chemokines. The results suggest that Tim-3 deficiency, specifically in macrophages, facilitates the expression of many chemokines and cytokines via upregulating TLR4/NF-κB signaling pathway.

4.9. ROS plays a critical role in macrophage Tim-3 deficiency-mediated necroptosis

Currently, it is uncertain whether ROS is an incidental byproduct or an essential factor in TNF-induced necroptosis. ROS production was associated with necroptosis and directly correlates with the expression of inflammatory signaling molecules, such as COX2 [51,52]. A substantial increase of COX2 protein expression was noted in Tim-3^{M-KO} mice (Fig. S3A). The analysis of ROS levels revealed a significant increase of ROS levels in Tim-3^{M-KO} mice as compared to WT mice (Fig. 10A). Nec-1 or GSK-872 could block ROS accumulation by suppressing necroptosis. To reveal the role of ROS in neutrophil necroptosis, the ROS levels in HL-60 cells were detected. Both, the supernatants of THP-1 macrophages and TNF-α trigger ROS production (Fig. 10B and Fig. S3B). The supernatants of Tim-3 knockdown macrophages significantly induced the ROS generation of HL-60 cells (Fig. 10B). RIP1 or RIP3 inhibition significantly decreased cellular ROS accumulation. These findings demonstrate that necroptosis induces the accumulation of intracellular ROS. To further demonstrate the function of ROS in Tim-3 knockdown macrophages, we conducted *in vitro* experiments using THP-1 cells. Upon LPS stimulation, ROS generation increased considerably in ShTim-3 cells (Fig. 10C). Furthermore, we observed that pretreatment with the TLR4 or NF-κB p65 inhibitor significantly decreased the amount of ROS (Fig. 10D). This results further confirms that Tim-3 suppressed inflammation by inhibiting TLR4/NF-κB signaling pathway.

To determine whether Tim-3 knockdown macrophages drive neutrophil necroptosis via ROS signaling or regulates necroptosis independently, we utilized the ROS scavenger N-acetyl-cysteine (NAC) to chelate ROS (Fig. 10E). Histological scores did not reveal noticeable differences in the colon of both WT and Tim-3^{M-KO} mice (Fig. 10F). The colon length and disease severity score were also not remarkably varied between the groups (Fig. 10G and H). Moreover, NAC treatment substantially reduced DSS-induced phosphorylation of RIP1, RIP3, and MLKL in Tim-3^{M-KO} mice (Fig. 10I). By performing immunofluorescence experiments, we found that *p*-MLKL was reduced in HL-60 cells pretreated with NAC (Fig. S3C). Note that in Tim-3 knockdown cells, the *p*-MLKL level was significantly downregulated in responding to NAC treatment (Fig. 10J). Therefore, it appears that macrophage Tim-3 regulates neutrophil necroptosis via an intracellular ROS signaling mechanism.

Collectively, these findings infer that ROS plays an important causative role in DSS-treated Tim-3^{M-KO} mice. On the one hand, ROS are downstream molecules of necroptosis, which activate necroptosis and enhance the pro-inflammatory effects. On the other hand, ROS may act as a signal transduction molecule and induce necroptosis.

4.10. Macrophage Tim-3 maintains the intestinal epithelial barrier by inhibiting neutrophil necroptosis

Considering that intestinal epithelial cells function as a major defensive barrier against luminal pathogens, we measured the expression of ZO-1 proteins and found that the expression level was significantly decreased in the colon of DSS-treated Tim-3^{M-KO} mice (Fig. 11A). We also observed a significant increase in tight junction proteins in the intestinal mucosa of Tim-3^{M-KO} mice with the administration of Nec-1 or GSK-872 compared with the vehicle-treated group (Fig. 11B).

To further study the underlying mechanism, an *in vitro* cell model was employed. Considering that the induction of neutrophil necroptosis provokes strong inflammatory responses, we determined whether the synergistic effect of Tim-3 knockdown macrophages and neutrophils further impairs barrier integrity. As shown in Fig. 11C–a macrophage or macrophage-neutrophil culture supernatant was added to the Caco2 cells. As expected, co-culture supernatant of Tim-3 knockdown macrophages and neutrophils resulted in more severe intestinal barrier damage (Fig. 11D–G). To further verify the substantial role of necroptosis in inducing intestinal barrier damage, neutralizing TNF-α antibodies were administrated into media from Tim-3 knockdown macrophages. The results showed that the decrease in ZO-1 by Tim-3 knockdown macrophages was abolished by neutralizing TNF-α antibodies (Fig. 11E–H).

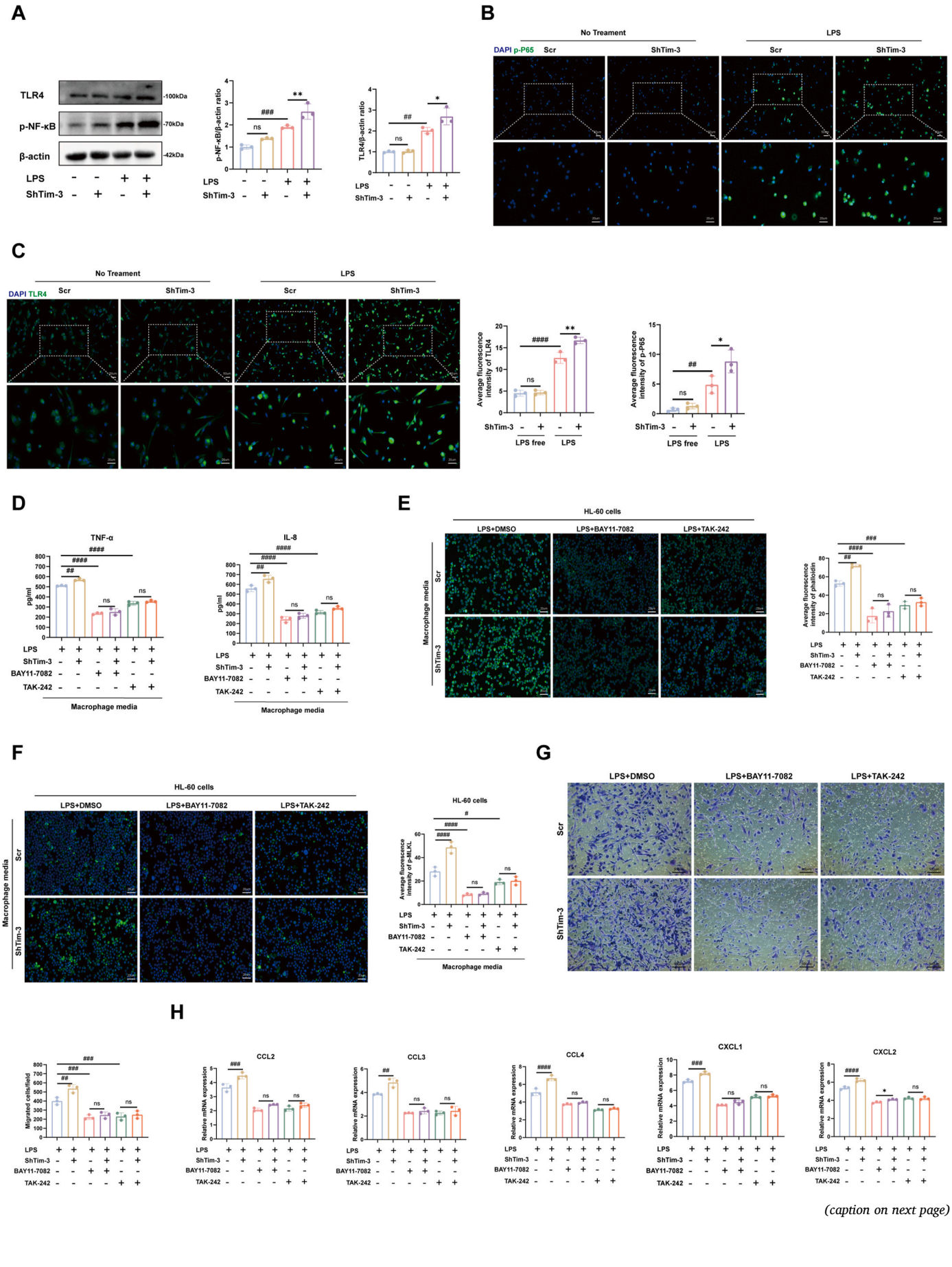

(caption on next page)

Fig. 9. Macrophage Tim-3 inhibits inflammatory responses via downregulating TLR4/NF-κB signaling pathway
(A-C) Control (Scr) and Tim-3 knockdown (ShTim-3) THP-1 cells were incubated in medium alone or medium containing LPS (400 ng/ml); then cells were collected at 6 h (n = 3). (A) Western blot analysis of p–NF–κB, TLR4, and β-actin from Scr or ShTim-3 THP-1 cells. (B, C) Representative immunofluorescence images stained for p–NF–κB and TLR4 (n = 3). Scale bars: 50 μm. (D–H) Scr and ShTim-3 THP-1 cells were incubated with LPS for 6 h. The THP-1 cells underwent pretreatment with the NF-κB inhibitor (50 μM BAY11-7082) or TLR4 inhibitor (50 μM TAK-242) for 30 min. The supernatant of THP-1 cells was harvested and added to HL-60 cells (n = 3). (D) The supernatants of THP-1 cells were tested for TNF-α and IL-8. (E) Phalloidin staining of the actin cytoskeleton in HL-60 cells (n = 3 for each group). Scale bars: 20 μm. (F) Representative immunofluorescence images stained for *p*-MLKL in HL-60 cells (n = 3 for each group). Scale bars: 20 μm. (G) Representative images of Scr and ShTim-3 THP-1 cells transwell migration (n = 3). Scale bars: 500 μm. (H) qRT-PCR results of CCL2, CCL3, CCL4, CXCL1 and CXCL2 in Scr and ShTim-3 THP-1 cells (n = 3 for each group). Data are presented as the mean ± SD. $^{*}P < 0.05$, $^{**}P < 0.01$; $\#P < 0.05$, $\#\#P < 0.01$, $\#\#\#P < 0.001$, $\#\#\#\#P < 0.0001$; ns, no significance.

Meanwhile, the decrease in ZO-1 protein due to macrophage Tim-3 deficiency was increased by Nec-1 or GSK-872 (Fig. 11F–I). These findings demonstrate that macrophage Tim-3 maintains the intestinal epithelial barrier via downregulating neutrophil necroptosis.

Necroptosis may lead to rapid plasma membrane permeabilization and exposure of danger associated molecular patterns proteins (DAMPs), resulting in intestinal inflammation and immune injury [20,53–55]. HMGB1 has been reported as a major DAMP released during necroptosis [56–58]. ELISA was conducted to detect the HMGB1 protein level in the macrophage or macrophage-neutrophil culture supernatant. We observed a significant increase in HMGB1 proteins in the co-culture supernatant of Tim-3 knockdown macrophages and neutrophils (Fig. 11J and K). Compared with the negative controls, the Tim-3 knockdown cells displayed higher levels of HMGB1 protein than NC cells, which experienced a reduction by Nec-1, or GSK-872 (Fig. 11H). The results demonstrate an important role of necroptosis-released DAMPs in disrupting the intestinal epithelial barrier. Collectively, our data proved that Tim-3 knockdown macrophages and neutrophils share cooperative effector activities during inflammation, which may amplify the inflammatory response, contributing to gut barrier disruption.

5. Discussion

In this study, we examined the roles of macrophage Tim-3 in experimental colitis using macrophage Tim-3 deficiency mice. The functional impacts and underlying mechanisms of Tim-3 in macrophage-linked inflammation were examined both *in vivo* and *in vitro*. This study is the first to provide evidence of macrophage Tim-3 alleviating colitis by inhibiting neutrophil necroptosis. The principal findings of this study are as follows: (1) Tim-3 expression in macrophages is upregulated in IBD tissue; (2) macrophage Tim-3 deficiency promotes M1 polarization, increases pro-inflammatory mediator expression and macrophage/neutrophil recruitment, and exacerbates colitis; (3) macrophage Tim-3 deficiency promotes colon inflammation by upregulating necroptosis signaling; (4) Tim-3 deficient macrophages induce neutrophil recruitment and trigger necroptosis; (5) macrophage Tim-3 inhibits downstream signaling pathways via downregulating TLR4/NF-κB signaling pathway; (6) macrophage Tim-3 maintains intestinal epithelial barrier by reducing necroptosis-released HMGB1. Collectively, our findings affirm the significance of macrophage Tim-3 as a critical modulator of neutrophil necroptosis in colitis.

Tim-3 functions as a checkpoint for the activation of T cells and is involved in the regulation of cytokine release, apoptotic body capture, and cell activation, facilitating the progression of many diseases [59,60]. Although the function of Tim-3 in T cells has been demonstrated [61,62], the mechanism of macrophage Tim-3 remains ambiguous and requires further study. To date, there have been several reports of Tim-3 in patients with IBD [63–65]. Our previous study also highlighted the involvement of Tim-3 in IBD [46]. Overall, all data indicate that Tim-3 plays a protective role in IBD. However, reports on Tim-3 expression were inconsistent in IBD patients. To characterize macrophage Tim-3 expression in experimental colitis and patients with IBD, we performed a series of experiments.

Although macrophage Tim-3 is not abundant in the colonic mucosa, it plays an important role as a signaling molecule. Macrophages are essential innate immune cells that engage in the development of UC at different activation levels and polarization states [66–68]. Macrophages are also central regulators of T-cell activation; therefore, targeting macrophages to suppress inflammatory reactions may provide an attractive therapeutic option for patients with UC [69]. UC is linked to chronic inflammation, which may result from an aberrant immune response toward intestinal microbiota and/or food antigens [16]. Generally, it is accepted that UC is linked to the Th2 pattern of inflammation, with the intestinal flora suspected to play an important role [34,70]. That is, the intestinal macrophages exhibit an immune response that depends on the gut microbiota, affecting macrophage polarization [71]. Therefore, we characterized the function and mechanism of action of macrophage Tim-3 in patients with UC. In this study, we affirmed an increase in GATA3 and MPO expression in Tim-3^{M-KO} mice without DSS treatment. This indicated that Tim-3^{M-KO} mice had a greatly increased propensity to develop colitis compared with WT mice.

Next, we determined how macrophage Tim-3 activates the downstream signal pathway in colitis. Previous studies proposed Tim-3 as a modulator of pro-as well as anti-inflammatory innate immune responses. For instance, Yang et al. reported that upregulated Tim-3 expression levels in macrophages substantially suppress TLR4-mediated NF-κB activation and pro-inflammatory cytokine secretion [47]. We have previously reported that Tim-3 is closely associated with the TLR4/NF-κB signaling pathway. In the present study, macrophage Tim-3 deficiency increased expression of TLR4/NF-κB upregulated inflammatory cytokines (e.g., TNF-α and IL-8) and chemokines, and enhanced migratory capacity, leading to excessive inflammatory immune responses. Our results, for the first time, illustrate that macrophage Tim-3 suppresses the migratory capacity of macrophages via downregulation of the TLR4/NF-κB signaling pathway.

To further elucidate the mechanism of how Tim-3 deficiency macrophages affect inflammatory response, we conducted RNA sequencing. In the pathway enrichment, the tumor necrosis factor pathway was significantly enriched in DSS-treated Tim-3^{M-KO} mice. In the present study, TNF-α expression was significantly induced in Tim-3 knockdown macrophages. In macrophages, TNF-α can trigger the production of TNF-α itself and IL-1β [72]; therefore, we focused on the interrelation between Tim-3 and TNF-α. High concentrations of cytokines (e.g., TNF-α), oxidative stress, the FAS ligand activation pathway, and endoplasmic

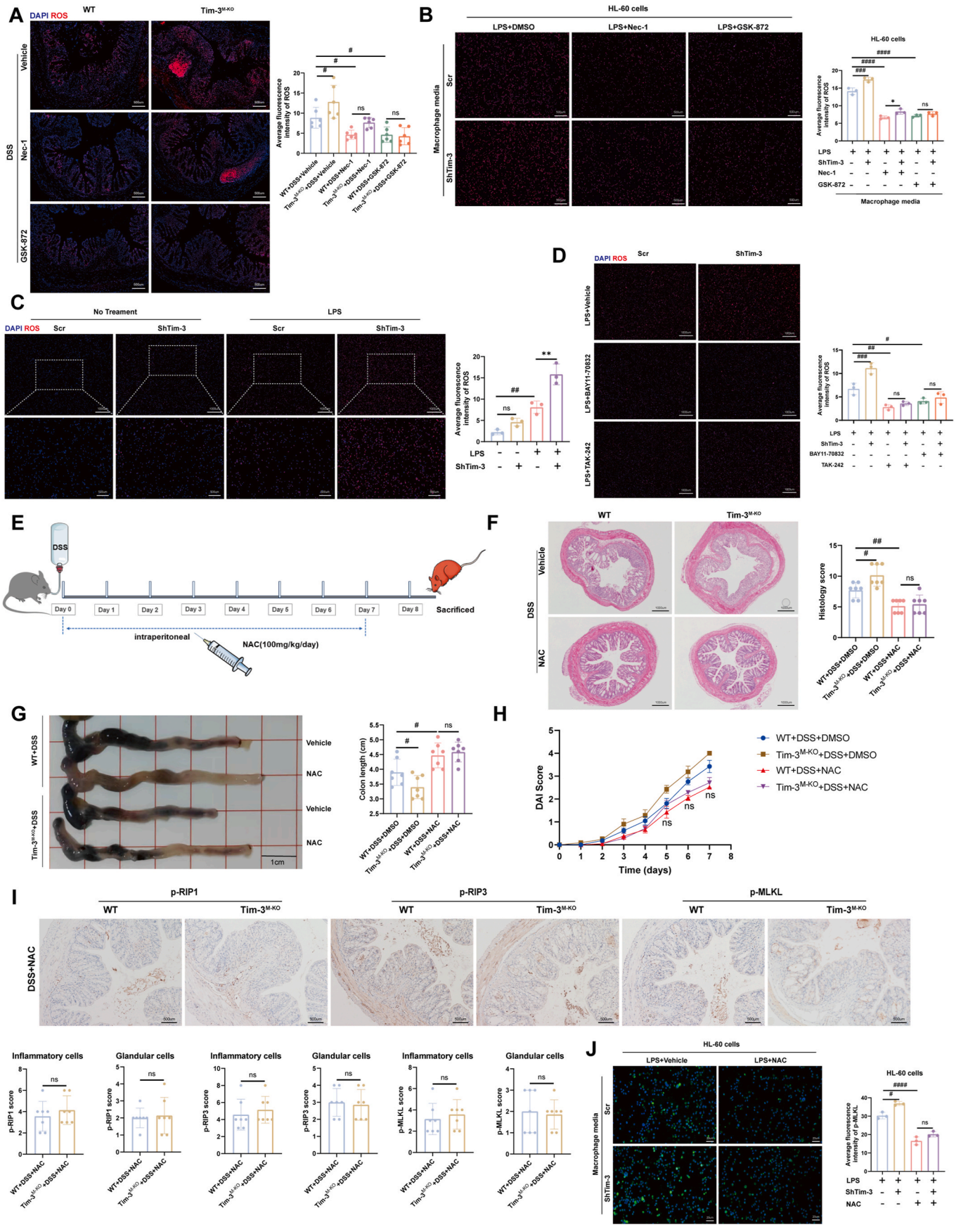

(caption on next page)

Fig. 10. ROS plays a critical role in macrophage Tim-3 deficiency-mediated necroptosis.
(A) DHE staining to evaluate ROS levels in colonic tissues of WT and Tim-3^{M-KO} mice (n = 6 for each group). Scale bars: 500 μm. (B–D) Representative pictures of ROS levels in the HL-60 cells (B) and THP-1 cells (C, D). Intracellular ROS levels were examined using DHE staining (n = 3). Scale bars: 1000 μm. (E) Study design of the experiment. Mice were intraperitoneally treated with either the vehicle control or N-Acetyl-Cysteine (NAC) (100 mg/kg/day) throughout the entire experimental period. n = 7 mice per group. (F) Representative diagram for the H&E staining of colon cross-sections. Histological analysis of the colon tissue. Scale bars: 1000 μm. n = 7 mice per group. (G) Representative images of mouse colons. n = 7 mice per group. (H) DAI of mice was documented daily. n = 7 mice per group. (I) Immunohistochemical staining of p-RIP1, p-RIP3, and *p*-MLKL in colonic tissues from DSS-treated mice with or without NAC administration. The quantification of the relative number of positive cells is shown in the graph below (n = 7). Scale bars: 500 μm. (J) Representative image of the immunofluorescence assay result for anti-*p*-MLKL (green) and DAPI (blue) staining, and quantitative analyses were performed using ImageJ (n = 3). Data are presented as mean ± SD except for those in Fig. 10H, which are presented as mean ± SEM. $^{*}P < 0.05$, $^{**}P < 0.01$; $\#\#P < 0.01$, $\#\#\#P < 0.001$, $\#\#\#\#P < 0.0001$; ns, no significance.

reticulum stress can lead to necroptosis [73,74]. Due to external stimuli and challenges, the intestinal tract undergoes programmed death processes other than apoptosis, such as necroptosis, autophagy, pyroptosis, and ferroptosis [75]. Routinely utilized TUNEL assays detected fragmented DNA linked to apoptotic cells [76]. Contrastingly, no significant difference was observed between the Tim-3^{M-KO} and WT groups. Based on our results and related literature, we speculate that macrophage Tim-3 can affect the inflammatory response by reducing TNF-α secretion.

This study, to the best of our knowledge, for the first time reported the necroptosis role of neutrophils in IBD. We speculate that the TNF-α is an important media of communication between Tim-3 knockdown macrophages and neutrophil necroptosis. It has been shown that neutrophil necroptosis is triggered by the stimulation of TNF-α, the ligation of adhesion receptors, the exposure to monosodium urate (MSU) crystals, or the phagocytosis of *Staphylococcus aureus* [77]. A previous study has examined the induction of necroptosis and found that neutrophil migration to inflammatory sites activates the RIP3-MLKL pathway [78]. Macrophages and neutrophils are important partners in innate immunity, hence, understanding macrophage–neutrophil interactions will provide insight into the regulation of IBD [79]. Neutrophil cryptitis and crypt abscesses are key pathogenic events in UC [80]. Impairment of the function of the intestinal barrier can predispose the immune cells in the lamina propria to enteric bacteria, which can promote neutrophil accumulation and consequently induce inflammation [81]. Herein, we discovered that treatment with Nec-1 or GSK-872 effectively attenuates gut inflammation. A double immunofluorescence experiment was conducted to demonstrate that necroptosis primarily occurs in neutrophils after Tim-3 knockdown in macrophages. Thus, macrophage Tim-3 is a critical regulator of inflammatory responses in neutrophils.

An important finding of this study is the high level of ROS in DSS-treated Tim-3^{M-KO} mice. Du et al. demonstrated that Tim-3 is a central negative modulator of ROS as well as inflammation in macrophages, alleviating hepatic injury in nonalcoholic steatohepatitis (NASH) mice [82]. Numerous studies have revealed that TLR4/NF-κB signaling pathway plays a key role in mediating ROS production [83–86]. In the present study, we found that macrophage Tim-3 decreased ROS via TLR4/NF-κB signaling pathway. The result suggested that macrophage Tim-3 may exerted an anti-inflammatory effect through regulating ROS generation, which in turn inhibits signaling cascades that avoid the release of the inflammatory response factors TNF-α and IL-8. Neutrophils promote gut inflammation by producing high levels of ROS, impair the epithelial barrier, and promote redox-sensitive inflammatory pathways [5,6]. The phosphorylation of MLKL by RIP1/3 in TNF-induced necroptosis was shown to result in the generation of ROS [87]. As a result, TNF-induced mitochondrial ROS production was inhibited in cells lacking RIP1/3 or MLKL, preventing them from undergoing necroptosis [87,88]. Here we discovered treatment with Nec-1 or GSK-872 effectively reduced the elevated ROS levels of neutrophils. Basit et al. reported that ROS is both an upstream activator and a downstream target of necroptosis [89]. Some studies have inferred that ROS overproduction functions critically in programmed cell death, disrupting cell components, enhancing RIP1 autophosphorylation, and triggering necroptosis [90,91]. TNF-α regulates the immune system by causing activation of the TNF-α receptors and downstream pathways that involve molecules like ROS [92,93]. NAC treatment can promote mitochondrial integrity via many mechanisms, maintains the function of mitochondria, and reduces ROS synthesis, hence protecting the cells from necroptosis [94]. In our study, NAC treatment markedly suppressed necroptosis and pro-inflammatory cytokine production in Tim-3^{M-KO} mice, and the results showed that neutrophil necroptosis could be inhibited by NAC. Therefore, based on the results of this study and those of previous studies, we speculate that ROS play a significant causative role in DSS-treated Tim-3^{M-KO} mice.

Another important finding of this study is the relationship between necroptosis and the intestinal epithelial barrier. A compromised mucosal barrier and intestinal epithelial damage are pathognomonic of IBD. Necroptosis is a programmed cell death pathway that regulates inflammation and immune responses through the release of DAMPs [95,96]. Released extracellular HMGB1 acts as a DAMPs signal, which is an alarming signal, and the released HMGB1 induces a signal cascade and promotes the release of several inflammatory factors [21]. HMGB1 and B box can increase the permeability of intestinal epithelia and impair the intestinal barrier [97]. Both *in vitro* and *in vivo* studies demonstrated that macrophage Tim-3 can effectively attenuate neutrophil necroptosis and inhibit the release of HMGB1 in neutrophil. Based on this, we speculate that macrophage Tim-3 maintains the intestinal epithelial barrier by inhibiting the generation of HMGB1 in neutrophils. Characterizing the neutrophil necroptosis signaling pathway may allow for better control of tissue damage or inflammation caused by neutrophil dysfunction.

To the best of our knowledge, this study is the first to demonstrate the involvement of macrophages in modulating necroptosis of neutrophils. Although these findings are novel, this study has some limitations. Our data suggest that HMGB1 release by neutrophils could severely disrupt the intestinal mucosal barrier in DSS-treated Tim-3^{M-KO} mice. The mechanisms underlying the interplay of necroptosis neutrophils and intestinal epithelial cells are complex and not completely resolved. Further studies are therefore required to elucidate the precise stimulatory mechanisms.

In conclusion, this study showed that Tim-3 knockdown macrophages release chemokines that attract neutrophils and, subsequently,

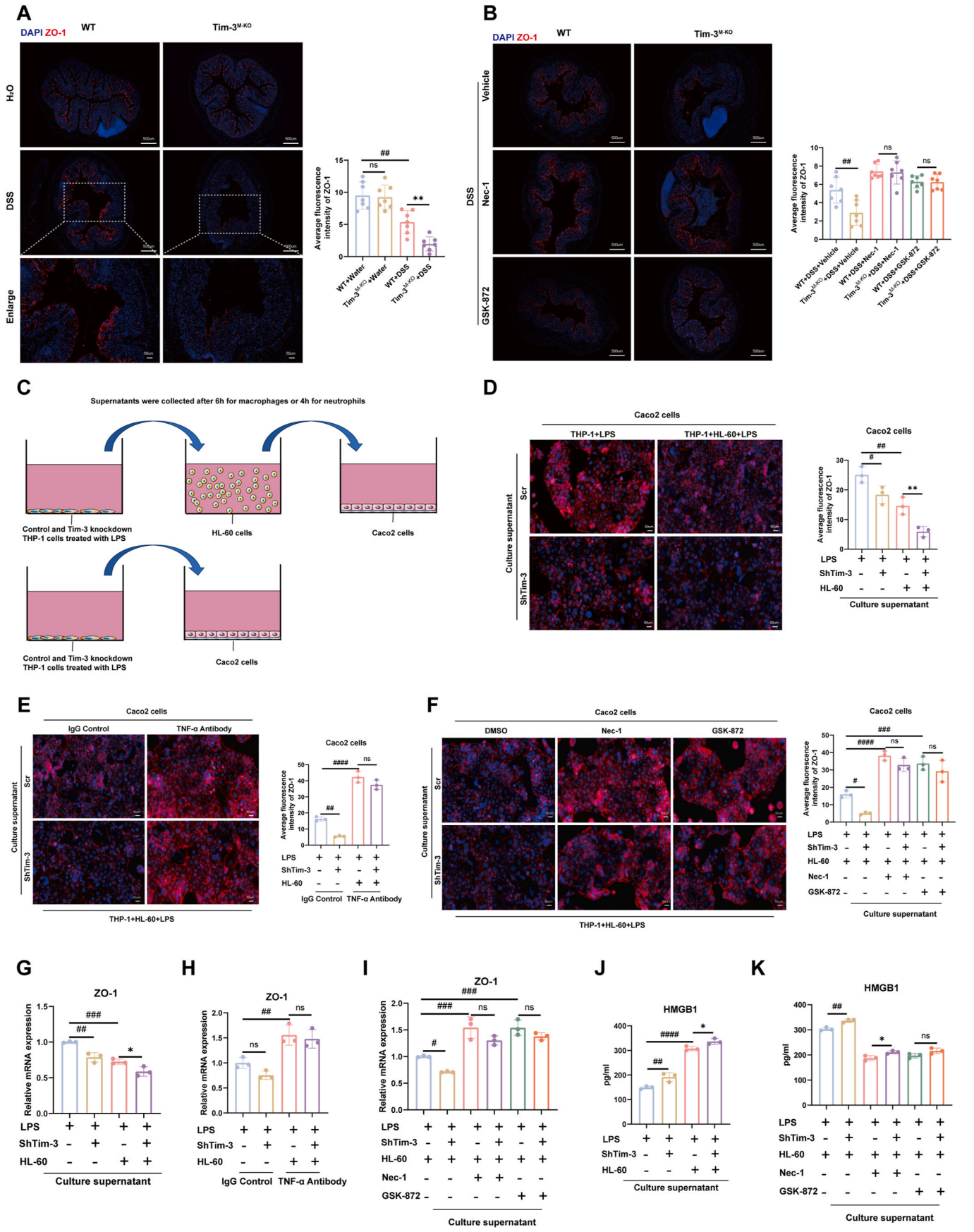

(caption on next page)

Fig. 11. Macrophage Tim-3 maintains the intestinal epithelial barrier by inhibiting neutrophil necroptosis
(A, B) Immunofluorescence staining of ZO-1 in mouse colonic tissue isolated from WT and Tim-3^{M-KO} mice with or without DSS treatment. n = 7 mice per group. (C) Study design. The experiments were divided into two groups: THP-1 + HL-60 + Caco2 cells and THP-1 + Caco2 cells. Scr or ShTim-3 THP-1 cells were incubated with LPS. The upper panel shows that the supernatants of THP-1 cells were harvested and added to HL-60 cells; then, the supernatants of the co-culture medium (THP-1 + HL-60 cells) added to Caco2 cells (THP-1 + HL-60 + Caco2 cells). The lower panel shows the supernatants of THP-1 cells were harvested and added to Caco-2 cells (THP-1 + Caco2 cells). The supernatant of Scr or ShTim-3 THP-1 cells underwent pretreatment with isotype control or anti-TNF-α antibody and added to HL-60 cells. The HL-60 cells underwent pretreatment with the RIP1 inhibitor (30 μM Nec-1) or RIP3 inhibitor (50 μM GSK-872) for 30 min. (D–F) Representative immunofluorescence images stained for ZO-1 in Caco2 cells (n = 3 for each group). Scale bars: 20 μm. (G–I) qRT-PCR results of ZO-1 in Caco2 cells (n = 3 for each group). (J, K) The supernatants of THP-1 cells or the co-culture medium (THP-1 cells + HL-60 cells) were tested for HMGB1. Data are presented as the mean ± SD. $^{**}P < 0.01$, $^{***}P < 0.001$; $\#\#P < 0.01$, $\#\#\#P < 0.001$, $\#\#\#\#P < 0.0001$; ns, no significance.

secrete TNF-α to induce neutrophil necroptosis. These findings provide novel insights into the pathophysiology of UC and the function of Tim-3 in mediating interactions between macrophages and neutrophils.

Funding

Funding was provided by grants from the National Natural Science Foundation of China (Nos. 81760105, 82060108 and 82260111).

Ethics statement

The ethics committee of The First Affiliated Hospital of Nanchang University approved the study. The ethic numbers are (2022)CDYFYYLK (06-021) and CDYFY-IACUC-202301QR046.

CRediT authorship contribution statement

Fangfei Wang: Writing – review & editing, Writing – original draft, Visualization, Validation, Supervision, Project administration, Methodology, Investigation, Funding acquisition, Formal analysis, Data curation. **Feng Zhou:** Supervision, Software, Data curation. **Jianxiang Peng:** Methodology, Investigation, Formal analysis. **Hao Chen:** Project administration, Methodology. **Jinliang Xie:** Software, Project administration, Methodology, Conceptualization. **Cong Liu:** Resources, Methodology. **Huifang Xiong:** Funding acquisition, Formal analysis. **Sihai Chen:** Validation, Software, Conceptualization. **Guohui Xue:** Supervision, Resources, Investigation, Funding acquisition. **Xiaojiang Zhou:** Supervision, Formal analysis. **Yong Xie:** Supervision, Resources, Funding acquisition, Formal analysis.

Declaration of competing interest

The authors declare that they have no known competing financial interests or personal relationships that could have appeared to influence the work reported in this paper.

Data availability

Data will be made available on request.

Acknowledgments

Our gratitude extends to the Science and Technology Projects of Jiangxi Province (No. 20201ZDG02007) for their valuable support in this endeavor.

Appendix A. Supplementary data

Supplementary data to this article can be found online at https://doi.org/10.1016/j.redox.2024.103072.

References

[1] R. Hodson, Inflammatory bowel disease, Nature 540 (7634) (2016) S97, https://doi.org/10.1038/540S97a.
[2] B. Khor, A. Gardet, R.J. Xavier, Genetics and pathogenesis of inflammatory bowel disease, Nature 474 (7351) (2011) 307–317, https://doi.org/10.1038/nature10209.
[3] C. Abraham, J.H. Cho, Inflammatory bowel disease, N. Engl. J. Med. 361 (21) (2009) 2066–2078, https://doi.org/10.1056/NEJMra0804647.
[4] M. Dave, K.A. Papadakis, W.A. Faubion Jr., Immunology of inflammatory bowel disease and molecular targets for biologics, Gastroenterol. Clin. N. Am. 43 (3) (2014) 405–424, https://doi.org/10.1016/j.gtc.2014.05.003.
[5] O. Wéra, P. Lancellotti, C. Oury, The dual role of neutrophils in inflammatory bowel diseases, J. Clin. Med. 5 (12) (2016), https://doi.org/10.3390/jcm5120118.
[6] G.X. Zhou, Z.J. Liu, Potential roles of neutrophils in regulating intestinal mucosal inflammation of inflammatory bowel disease, Journal of digestive diseases 18 (9) (2017) 495–503, https://doi.org/10.1111/1751-2980.12540.
[7] C. Caër, M.J. Wick, Human intestinal mononuclear phagocytes in Health and inflammatory bowel disease, Front. Immunol. 11 (2020) 410, https://doi.org/10.3389/fimmu.2020.00410.
[8] A.M. Hine, P. Loke, Intestinal macrophages in resolving inflammation, J. Immunol. 203 (3) (2019) 593–599, https://doi.org/10.4049/jimmunol.1900345.
[9] Y. Lavin, A. Mortha, A. Rahman, M. Merad, Regulation of macrophage development and function in peripheral tissues, Nat. Rev. Immunol. 15 (12) (2015) 731–744, https://doi.org/10.1038/nri3920.
[10] L. Monney, C.A. Sabatos, J.L. Gaglia, A. Ryu, H. Waldner, T. Chernova, et al., Th1-specific cell surface protein Tim-3 regulates macrophage activation and severity of an autoimmune disease, Nature 415 (6871) (2002) 536–541, https://doi.org/10.1038/415536a.
[11] W.D. Hastings, D.E. Anderson, N. Kassam, K. Koguchi, E.A. Greenfield, S.C. Kent, et al., TIM-3 is expressed on activated human CD4+ T cells and regulates Th1 and Th17 cytokines, Eur. J. Immunol. 39 (9) (2009) 2492–2501, https://doi.org/10.1002/eji.200939274.
[12] A.C. Anderson, D.E. Anderson, L. Bregoli, W.D. Hastings, N. Kassam, C. Lei, et al., Promotion of tissue inflammation by the immune receptor Tim-3 expressed on innate immune cells, Science (New York, NY) 318 (5853) (2007) 1141–1143, https://doi.org/10.1126/science.1148536.
[13] Y. Ju, N. Hou, J. Meng, X. Wang, X. Zhang, D. Zhao, et al., T cell immunoglobulin- and mucin-domain-containing molecule-3 (Tim-3) mediates natural killer cell suppression in chronic hepatitis B, J. Hepatol. 52 (3) (2010) 322–329, https://doi.org/10.1016/j.jhep.2009.12.005.
[14] S. Nakae, M. Iikura, H. Suto, H. Akiba, D.T. Umetsu, R.H. Dekruyff, et al., TIM-1 and TIM-3 enhancement of Th2 cytokine production by mast cells, Blood 110 (7) (2007) 2565–2568, https://doi.org/10.1182/blood-2006-11-058800.
[15] M. Khademi, Z. Illés, A.W. Gielen, M. Marta, N. Takazawa, C. Baecher-Allan, et al., T Cell Ig- and mucin-domain-containing molecule-3 (TIM-3) and TIM-1 molecules are differentially expressed on human Th1 and Th2 cells and in cerebrospinal fluid-derived mononuclear cells in multiple sclerosis, J. Immunol. 172 (11) (2004) 7169–7176, https://doi.org/10.4049/jimmunol.172.11.7169.
[16] A. Kałużna, P. Olczyk, K. Komosińska-Vassev, The role of innate and adaptive immune cells in the pathogenesis and development of the inflammatory response in ulcerative colitis, J. Clin. Med. 11 (2) (2022), https://doi.org/10.3390/jcm11020400.
[17] A. Saez, B. Herrero-Fernandez, R. Gomez-Bris, H. Sánchez-Martinez, J. M. Gonzalez-Granado, Pathophysiology of inflammatory bowel disease: innate immune system, Int. J. Mol. Sci. 24 (2) (2023), https://doi.org/10.3390/ijms24021526.
[18] M. Pasparakis, P. Vandenabeele, Necroptosis and its role in inflammation, Nature 517 (7534) (2015) 311–320, https://doi.org/10.1038/nature14191.
[19] R. Weinlich, A. Oberst, H.M. Beere, D.R. Green, Necroptosis in development, inflammation and disease, Nat. Rev. Mol. Cell Biol. 18 (2) (2017) 127–136, https://doi.org/10.1038/nrm.2016.149.
[20] A. Kaczmarek, P. Vandenabeele, D.V. Krysko, Necroptosis: the release of damage-associated molecular patterns and its physiological relevance, Immunity 38 (2) (2013) 209–223, https://doi.org/10.1016/j.immuni.2013.02.003.
[21] P. Scaffidi, T. Misteli, M.E. Bianchi, Release of chromatin protein HMGB1 by necrotic cells triggers inflammation, Nature 418 (6894) (2002) 191–195, https://doi.org/10.1038/nature00858.
[22] K.D. Marshall, C.P. Baines, Necroptosis: is there a role for mitochondria? Front. Physiol. 5 (2014) 323, https://doi.org/10.3389/fphys.2014.00323.
[23] S. Fulda, Regulation of necroptosis signaling and cell death by reactive oxygen species, Biol. Chem. 397 (7) (2016) 657–660, https://doi.org/10.1515/hsz-2016-0102.
[24] M.E. Choi, D.R. Price, S.W. Ryter, A.M.K. Choi, Necroptosis: a crucial pathogenic mediator of human disease, JCI insight 4 (15) (2019), https://doi.org/10.1172/jci.insight.128834.

[25] M. Dannappel, K. Vlantis, S. Kumari, A. Polykratis, C. Kim, L. Wachsmuth, et al., RIPK1 maintains epithelial homeostasis by inhibiting apoptosis and necroptosis, Nature 513 (7516) (2014) 90–94, https://doi.org/10.1038/nature13608.

[26] G. Zhou, L. Yu, L. Fang, W. Yang, T. Yu, Y. Miao, et al., CD177(+) neutrophils as functionally activated neutrophils negatively regulate IBD, Gut 67 (6) (2018) 1052–1063, https://doi.org/10.1136/gutjnl-2016-313535.

[27] A. Bressenot, J. Salleron, C. Bastien, S. Danese, C. Boulagnon-Rombi, L. Peyrin-Biroulet, Comparing histological activity indexes in UC, Gut 64 (9) (2015) 1412–1418, https://doi.org/10.1136/gutjnl-2014-307477.

[28] F. Biasi, G. Leonarduzzi, P.I. Oteiza, G. Poli, Inflammatory bowel disease: mechanisms, redox considerations, and therapeutic targets, Antioxidants Redox Signal. 19 (14) (2013) 1711–1747, https://doi.org/10.1089/ars.2012.4530.

[29] K. De Filippo, A. Dudeck, M. Hasenberg, E. Nye, N. van Rooijen, K. Hartmann, et al., Mast cell and macrophage chemokines CXCL1/CXCL2 control the early stage of neutrophil recruitment during tissue inflammation, Blood 121 (24) (2013) 4930–4937, https://doi.org/10.1182/blood-2013-02-486217.

[30] T. Kucharzik, P. Ellul, T. Greuter, J.F. Rahier, B. Verstockt, C. Abreu, et al., ECCO guidelines on the prevention, diagnosis, and management of infections in inflammatory bowel disease, Journal of Crohn's & colitis 15 (6) (2021) 879–913, https://doi.org/10.1093/ecco-jcc/jjab052.

[31] S. Wirtz, C. Neufert, B. Weigmann, M.F. Neurath, Chemically induced mouse models of intestinal inflammation, Nat. Protoc. 2 (3) (2007) 541–546, https://doi.org/10.1038/nprot.2007.41.

[32] A. Millius, O.D. Weiner, Chemotaxis in neutrophil-like HL-60 cells, Methods Mol. Biol. 571 (2009) 167–177, https://doi.org/10.1007/978-1-60761-198-1_11.

[33] G. Xue, H. Xiong, S. Wang, Y. Fu, Y. Xie, Eudragit-coated chitosan-tripterygium glycoside conjugate microspheres alleviate DSS-induced experimental colitis by inhibiting the TLR4/NF-κB signaling pathway, Biomedicine & pharmacotherapy = Biomedecine & pharmacotherapie 158 (2023) 114194, https://doi.org/10.1016/j.biopha.2022.114194.

[34] A. Geremia, P. Biancheri, P. Allan, G.R. Corazza, A. Di Sabatino, Innate and adaptive immunity in inflammatory bowel disease, Autoimmun. Rev. 13 (1) (2014) 3–10, https://doi.org/10.1016/j.autrev.2013.06.004.

[35] S. He, L. Wang, L. Miao, T. Wang, F. Du, L. Zhao, et al., Receptor interacting protein kinase-3 determines cellular necrotic response to TNF-alpha, Cell 137 (6) (2009) 1100–1111, https://doi.org/10.1016/j.cell.2009.05.021.

[36] Z. Liu, L.F. Dagley, K. Shield-Artin, S.N. Young, A. Bankovacki, X. Wang, et al., Oligomerization-driven MLKL ubiquitylation antagonizes necroptosis, EMBO J. 40 (23) (2021) e103718, https://doi.org/10.15252/embj.2019103718.

[37] Z. Cai, S. Jitkaew, J. Zhao, H.C. Chiang, S. Choksi, J. Liu, et al., Plasma membrane translocation of trimerized MLKL protein is required for TNF-induced necroptosis, Nat. Cell Biol. 16 (1) (2014) 55–65, https://doi.org/10.1038/ncb2883.

[38] M.B. Grisham, T. Yamada, Neutrophils, nitrogen oxides, and inflammatory bowel disease, Ann. N. Y. Acad. Sci. 664 (1992) 103–115, https://doi.org/10.1111/j.1749-6632.1992.tb39753.x.

[39] Y.R. Na, M. Stakenborg, S.H. Seok, G. Matteoli, Macrophages in intestinal inflammation and resolution: a potential therapeutic target in IBD, Nat. Rev. Gastroenterol. Hepatol. 16 (9) (2019) 531–543, https://doi.org/10.1038/s41575-019-0172-4.

[40] A.C. Chin, C.A. Parkos, Neutrophil transepithelial migration and epithelial barrier function in IBD: potential targets for inhibiting neutrophil trafficking, Ann. N. Y. Acad. Sci. 1072 (2006) 276–287, https://doi.org/10.1196/annals.1326.018.

[41] C.G. Mayne, C.B. Williams, Induced and natural regulatory T cells in the development of inflammatory bowel disease, Inflamm. Bowel Dis. 19 (8) (2013) 1772–1788, https://doi.org/10.1097/MIB.0b013e318281f5a3.

[42] C. Smids, C.S. Horjus Talabur Horje, P.J. Wahab, M.J. Groenen, S. Middendorp, E. G. van Lochem, On naivety of T cells in inflammatory bowel disease: a review, Inflamm. Bowel Dis. 21 (1) (2015) 167–172, https://doi.org/10.1097/mib.0000000000000221.

[43] M. Baggiolini, I. Clark-Lewis, Interleukin-8, a chemotactic and inflammatory cytokine, FEBS Lett. 307 (1) (1992) 97–101, https://doi.org/10.1016/0014-5793(92)80909-z.

[44] N. Mukaida, A. Harada, K. Matsushima, Interleukin-8 (IL-8) and monocyte chemotactic and activating factor (MCAF/MCP-1), chemokines essentially involved in inflammatory and immune reactions, Cytokine Growth Factor Rev. 9 (1) (1998) 9–23, https://doi.org/10.1016/s1359-6101(97)00022-1.

[45] G. Servant, O.D. Weiner, P. Herzmark, T. Balla, J.W. Sedat, H.R. Bourne, Polarization of chemoattractant receptor signaling during neutrophil chemotaxis, Science (New York, NY) 287 (5455) (2000) 1037–1040, https://doi.org/10.1126/science.287.5455.1037.

[46] H. Xiong, G. Xue, Y. Zhang, S. Wu, Q. Zhao, R. Zhao, et al., Effect of exogenous galectin-9, a natural TIM-3 ligand, on the severity of TNBS- and DSS-induced colitis in mice, Int. Immunopharm. 115 (2023) 109645, https://doi.org/10.1016/j.intimp.2022.109645.

[47] X. Yang, X. Jiang, G. Chen, Y. Xiao, S. Geng, C. Kang, et al., T cell Ig mucin-3 promotes homeostasis of sepsis by negatively regulating the TLR response, J. Immunol. 190 (5) (2013) 2068–2079, https://doi.org/10.4049/jimmunol.1202661.

[48] Y. Uchida, B. Ke, M.C. Freitas, H. Yagita, H. Akiba, R.W. Busuttil, et al., T-cell immunoglobulin mucin-3 determines severity of liver ischemia/reperfusion injury in mice in a TLR4-dependent manner, Gastroenterology 139 (6) (2010) 2195–2206, https://doi.org/10.1053/j.gastro.2010.07.003.

[49] J.W. Lee, J.W. Park, O.K. Kwon, H.J. Lee, H.G. Jeong, J.H. Kim, et al., NPS2143 inhibits MUC5AC and proinflammatory mediators in cigarette smoke extract (CSE)-Stimulated human airway epithelial cells, Inflammation 40 (1) (2017) 184–194, https://doi.org/10.1007/s10753-016-0468-2.

[50] J. Li, D. Tong, J. Liu, F. Chen, Y. Shen, Oroxylin A attenuates cigarette smoke-induced lung inflammation by activating Nrf2, Int. Immunopharm. 40 (2016) 524–529, https://doi.org/10.1016/j.intimp.2016.10.011.

[51] N. Vanlangenakker, T. Vanden Berghe, P. Bogaert, B. Laukens, K. Zobel, K. Deshayes, et al., cIAP1 and TAK1 protect cells from TNF-induced necrosis by preventing RIP1/RIP3-dependent reactive oxygen species production, Cell Death Differ. 18 (4) (2011) 656–665, https://doi.org/10.1038/cdd.2010.138.

[52] S. Reuter, S.C. Gupta, M.M. Chaturvedi, B.B. Aggarwal, Oxidative stress, inflammation, and cancer: how are they linked? Free Radic. Biol. Med. 49 (11) (2010) 1603–1616, https://doi.org/10.1016/j.freeradbiomed.2010.09.006.

[53] X. Hua, B. Li, F. Yu, W. Zhao, Y. Tan, X. Li, et al., Protective effect of MFG-E8 on necroptosis-induced intestinal inflammation and enteroendocrine cell function in diabetes, Nutrients 14 (3) (2022), https://doi.org/10.3390/nu14030604.

[54] S. Wen, X. Li, Y. Ling, S. Chen, Q. Deng, L. Yang, et al., HMGB1-associated necroptosis and Kupffer cells M1 polarization underlies remote liver injury induced by intestinal ischemia/reperfusion in rats, Faseb. J. : official publication of the Federation of American Societies for Experimental Biology 34 (3) (2020) 4384–4402, https://doi.org/10.1096/fj.201900817R.

[55] A. Negroni, E. Colantoni, M. Pierdomenico, F. Palone, M. Costanzo, S. Oliva, et al., RIP3 AND pMLKL promote necroptosis-induced inflammation and alter membrane permeability in intestinal epithelial cells, Dig. Liver Dis.: official journal of the Italian Society of Gastroenterology and the Italian Association for the Study of the Liver 49 (11) (2017) 1201–1210, https://doi.org/10.1016/j.dld.2017.08.017.

[56] L. Sun, H. Wang, Z. Wang, S. He, S. Chen, D. Liao, et al., Mixed lineage kinase domain-like protein mediates necrosis signaling downstream of RIP3 kinase, Cell 148 (1–2) (2012) 213–227, https://doi.org/10.1016/j.cell.2011.11.031.

[57] F. Humphries, S. Yang, B. Wang, P.N. Moynagh, RIP kinases: key decision makers in cell death and innate immunity, Cell Death Differ. 22 (2) (2015) 225–236, https://doi.org/10.1038/cdd.2014.126.

[58] U. Andersson, K.J. Tracey, HMGB1 is a therapeutic target for sterile inflammation and infection, Annu. Rev. Immunol. 29 (2011) 139–162, https://doi.org/10.1146/annurev-immunol-030409-101323.

[59] R. Ocaña-Guzman, L. Torre-Bouscoulet, I. Sada-Ovalle, TIM-3 regulates distinct functions in macrophages, Front. Immunol. 7 (2016) 229, https://doi.org/10.3389/fimmu.2016.00229.

[60] D. Zhao, M. Guo, B. Liu, Q. Lin, T. Xie, Q. Zhang, et al., Frontline Science: Tim-3-mediated dysfunctional engulfment of apoptotic cells in SLE, J. Leukoc. Biol. 102 (6) (2017) 1313–1322, https://doi.org/10.1189/jlb.3HI0117-005RR.

[61] L. Avery, J. Filderman, A.L. Szymczak-Workman, L.P. Kane, Tim-3 co-stimulation promotes short-lived effector T cells, restricts memory precursors, and is dispensable for T cell exhaustion, Proc. Natl. Acad. Sci. U.S.A. 115 (10) (2018) 2455–2460, https://doi.org/10.1073/pnas.1712107115.

[62] K.A. Lee, K.S. Shin, G.Y. Kim, Y.C. Song, E.A. Bae, I.K. Kim, et al., Characterization of age-associated exhausted CD8$^+$ T cells defined by increased expression of Tim-3 and PD-1, Aging Cell 15 (2) (2016) 291–300, https://doi.org/10.1111/acel.12435.

[63] M.J. Kim, W.Y. Lee, Y.H. Choe, Expression of TIM-3, human β-defensin-2, and FOXP3 and correlation with disease activity in pediatric Crohn's disease with infliximab therapy, Gut and liver 9 (3) (2015) 370–380, https://doi.org/10.5009/gnl13408.

[64] X. Jiang, J. Yu, Q. Shi, Y. Xiao, W. Wang, G. Chen, et al., Tim-3 promotes intestinal homeostasis in DSS colitis by inhibiting M1 polarization of macrophages, Clin. Immunol. 160 (2) (2015) 328–335, https://doi.org/10.1016/j.clim.2015.07.008.

[65] F. Shi, X. Guo, X. Jiang, P. Zhou, Y. Xiao, T. Zhou, et al., Dysregulated Tim-3 expression and its correlation with imbalanced CD4 helper T cell function in ulcerative colitis, Clin. Immunol. 145 (3) (2012) 230–240, https://doi.org/10.1016/j.clim.2012.09.001.

[66] X. Pan, Q. Zhu, L.L. Pan, J. Sun, Macrophage immunometabolism in inflammatory bowel diseases: from pathogenesis to therapy, Pharmacol. Therapeut. 238 (2022) 108176, https://doi.org/10.1016/j.pharmthera.2022.108176.

[67] M. Zhang, X. Li, Q. Zhang, J. Yang, G. Liu, Roles of macrophages on ulcerative colitis and colitis-associated colorectal cancer, Front. Immunol. 14 (2023) 1103617, https://doi.org/10.3389/fimmu.2023.1103617.

[68] K. Wang, T. Mao, X. Lu, M. Wang, Y. Yun, Z. Jia, et al., A potential therapeutic approach for ulcerative colitis: targeted regulation of macrophage polarization through phytochemicals, Front. Immunol. 14 (2023) 1155077, https://doi.org/10.3389/fimmu.2023.1155077.

[69] J.L. Guerriero, Macrophages: their untold story in T cell activation and function, International review of cell and molecular biology 342 (2019) 73–93, https://doi.org/10.1016/bs.ircmb.2018.07.001.

[70] V. Popp, K. Gerlach, S. Mott, A. Turowska, H. Garn, R. Atreya, et al., Rectal delivery of a DNAzyme that specifically blocks the transcription factor GATA3 and reduces colitis in mice, Gastroenterology 152 (1) (2017) 176, https://doi.org/10.1053/j.gastro.2016.09.005, 92.e5.

[71] J. Schulthess, S. Pandey, M. Capitani, K.C. Rue-Albrecht, I. Arnold, F. Franchini, et al., The short chain fatty acid butyrate imprints an antimicrobial program in macrophages, Immunity 50 (2) (2019) 432, https://doi.org/10.1016/j.immuni.2018.12.018, 45.e7.

[72] S. Hao, D. Baltimore, The stability of mRNA influences the temporal order of the induction of genes encoding inflammatory molecules, Nat. Immunol. 10 (3) (2009) 281–288, https://doi.org/10.1038/ni.1699.

[73] L.D. Santos, K.H. Antunes, S.P. Muraro, G.F. de Souza, A.G. da Silva, J.S. Felipe, et al., TNF-mediated alveolar macrophage necroptosis drives disease pathogenesis during respiratory syncytial virus infection, Eur. Respir. J. 57 (6) (2021), https://doi.org/10.1183/13993003.03764-2020.

[74] C.G. Weindel, E.L. Martinez, X. Zhao, C.J. Mabry, S.L. Bell, K.J. Vail, et al., Mitochondrial ROS promotes susceptibility to infection via gasdermin D-mediated

necroptosis, Cell 185 (17) (2022) 3214, https://doi.org/10.1016/j.cell.2022.06.038, 31.e23.
[75] N. Robinson, R. Ganesan, C. Hegedűs, K. Kovács, T.A. Kufer, L. Virág, Programmed necrotic cell death of macrophages: focus on pyroptosis, necroptosis, and parthanatos, Redox Biol. 26 (2019) 101239, https://doi.org/10.1016/j.redox.2019.101239.
[76] D.T. Loo, In situ detection of apoptosis by the TUNEL assay: an overview of techniques, Methods Mol. Biol. 682 (2011) 3–13, https://doi.org/10.1007/978-1-60327-409-8_1.
[77] X. Wang, S. Yousefi, H.U. Simon, Necroptosis and neutrophil-associated disorders, Cell Death Dis. 9 (2) (2018) 111, https://doi.org/10.1038/s41419-017-0058-8.
[78] X. Wang, Z. He, H. Liu, S. Yousefi, H.U. Simon, Neutrophil necroptosis is triggered by ligation of adhesion molecules following GM-CSF priming, J. Immunol. 197 (10) (2016) 4090–4100, https://doi.org/10.4049/jimmunol.1600051.
[79] C. Schulz, T. Petzold, H. Ishikawa-Ankerhold, Macrophage regulation of granulopoiesis and neutrophil functions, Antioxidants Redox Signal. 35 (3) (2021) 182–191, https://doi.org/10.1089/ars.2020.8203.
[80] K. Geboes, R. Riddell, A. Ost, B. Jensfelt, T. Persson, R. Löfberg, A reproducible grading scale for histological assessment of inflammation in ulcerative colitis, Gut 47 (3) (2000) 404–409, https://doi.org/10.1136/gut.47.3.404.
[81] L. Kang, X. Fang, Y.H. Song, Z.X. He, Z.J. Wang, S.L. Wang, et al., Neutrophil-epithelial crosstalk during intestinal inflammation, Cellular and molecular gastroenterology and hepatology 14 (6) (2022) 1257–1267, https://doi.org/10.1016/j.jcmgh.2022.09.002.
[82] X. Du, Z. Wu, Y. Xu, Y. Liu, W. Liu, T. Wang, et al., Increased Tim-3 expression alleviates liver injury by regulating macrophage activation in MCD-induced NASH mice, Cell. Mol. Immunol. 16 (11) (2019) 878–886, https://doi.org/10.1038/s41423-018-0032-0.
[83] Y. Wang, H. Hu, J. Yin, Y. Shi, J. Tan, L. Zheng, et al., TLR4 participates in sympathetic hyperactivity Post-MI in the PVN by regulating NF-κB pathway and ROS production, Redox Biol. 24 (2019) 101186, https://doi.org/10.1016/j.redox.2019.101186.
[84] A.P. West, I.E. Brodsky, C. Rahner, D.K. Woo, H. Erdjument-Bromage, P. Tempst, et al., TLR signalling augments macrophage bactericidal activity through mitochondrial ROS, Nature 472 (7344) (2011) 476–480, https://doi.org/10.1038/nature09973.
[85] A. Singh, V. Singh, R.L. Tiwari, T. Chandra, A. Kumar, M. Dikshit, et al., The IRAK-ERK-p67phox-Nox-2 axis mediates TLR4, 2-induced ROS production for IL-1β transcription and processing in monocytes, Cell. Mol. Immunol. 13 (6) (2016) 745–763, https://doi.org/10.1038/cmi.2015.62.
[86] Z. Jiang, J. Shen, J. Ding, Y. Yuan, L. Gao, Z. Yang, et al., USP18 mitigates lipopolysaccharide-induced oxidative stress and inflammation in human pulmonary microvascular endothelial cells through the TLR4/NF-κB/ROS signaling, Toxicol. Vitro : an international journal published in association with BIBRA 75 (2021) 105181, https://doi.org/10.1016/j.tiv.2021.105181.
[87] J. Zhao, S. Jitkaew, Z. Cai, S. Choksi, Q. Li, J. Luo, et al., Mixed lineage kinase domain-like is a key receptor interacting protein 3 downstream component of TNF-induced necrosis, Proc. Natl. Acad. Sci. U.S.A. 109 (14) (2012) 5322–5327, https://doi.org/10.1073/pnas.1200012109.
[88] F.J. Roca, L. Ramakrishnan, TNF dually mediates resistance and susceptibility to mycobacteria via mitochondrial reactive oxygen species, Cell 153 (3) (2013) 521–534, https://doi.org/10.1016/j.cell.2013.03.022.
[89] F. Basit, L.M. van Oppen, L. Schöckel, H.M. Bossenbroek, S.E. van Emst-de Vries, J. C. Hermeling, et al., Mitochondrial complex I inhibition triggers a mitophagy-dependent ROS increase leading to necroptosis and ferroptosis in melanoma cells, Cell Death Dis. 8 (3) (2017) e2716, https://doi.org/10.1038/cddis.2017.133.
[90] Y. Zhang, S.S. Su, S. Zhao, Z. Yang, C.Q. Zhong, X. Chen, et al., RIP1 autophosphorylation is promoted by mitochondrial ROS and is essential for RIP3 recruitment into necrosome, Nat. Commun. 8 (2017) 14329, https://doi.org/10.1038/ncomms14329.
[91] Y. Jia, F. Wang, Q. Guo, M. Li, L. Wang, Z. Zhang, et al., Curcumol induces RIPK1/RIPK3 complex-dependent necroptosis via JNK1/2-ROS signaling in hepatic stellate cells, Redox Biol. 19 (2018) 375–387, https://doi.org/10.1016/j.redox.2018.09.007.
[92] S. Grootjans, T. Vanden Berghe, P. Vandenabeele, Initiation and execution mechanisms of necroptosis: an overview, Cell Death Differ. 24 (7) (2017) 1184–1195, https://doi.org/10.1038/cdd.2017.65.
[93] H. Blaser, C. Dostert, T.W. Mak, D. Brenner, TNF and ROS crosstalk in inflammation, Trends Cell Biol. 26 (4) (2016) 249–261, https://doi.org/10.1016/j.tcb.2015.12.002.
[94] C.J. Li, L.Y. Sun, C.Y. Pang, Synergistic protection of N-acetylcysteine and ascorbic acid 2-phosphate on human mesenchymal stem cells against mitoptosis, necroptosis and apoptosis, Sci. Rep. 5 (2015) 9819, https://doi.org/10.1038/srep09819.
[95] R. Chen, R. Kang, D. Tang, The mechanism of HMGB1 secretion and release, Exp. Mol. Med. 54 (2) (2022) 91–102, https://doi.org/10.1038/s12276-022-00736-w.
[96] S.Y. Lin, S.Y. Hsieh, Y.T. Fan, W.C. Wei, P.W. Hsiao, D.H. Tsai, et al., Necroptosis promotes autophagy-dependent upregulation of DAMP and results in immunosurveillance, Autophagy 14 (5) (2018) 778–795, https://doi.org/10.1080/15548627.2017.1386359.
[97] P.L. Sappington, R. Yang, H. Yang, K.J. Tracey, R.L. Delude, M.P. Fink, HMGB1 B box increases the permeability of Caco-2 enterocytic monolayers and impairs intestinal barrier function in mice, Gastroenterology 123 (3) (2002) 790–802, https://doi.org/10.1053/gast.2002.35391.